REVIEW ARTICLE
https://doi.org/10.1038/s41563-019-0431-3

nature materials

Fundamentals of inorganic solid-state electrolytes for batteries

Theodosios Famprikis[1,2,3*], Pieremanuele Canepa[2,3,5], James A. Dawson[2,3], M. Saiful Islam[2,3*] and Christian Masquelier[1,3,4*]

In the critical area of sustainable energy storage, solid-state batteries have attracted considerable attention due to their potential safety, energy-density and cycle-life benefits. This Review describes recent progress in the fundamental understanding of inorganic solid electrolytes, which lie at the heart of the solid-state battery concept, by addressing key issues in the areas of multiscale ion transport, electrochemical and mechanical properties, and current processing routes. The main electrolyte-related challenges for practical solid-state devices include utilization of metal anodes, stabilization of interfaces and the maintenance of physical contact, the solutions to which hinge on gaining greater knowledge of the underlying properties of solid electrolyte materials.

The global trend towards decarbonization has led to research on battery materials taking centre stage as one of the key enabling technologies for the electrification of transport and the storage of intermittently produced solar and wind energy. In parallel, lithium-ion batteries have become ubiquitous by powering the revolution in portable electronics. However, the proliferation of electrochemical energy storage for applications of ever-increasing scale, such as electromobility and grid storage, hinges on strict performance, safety, energy density and cost requirements for the batteries of the future, which cannot necessarily be satisfied by the current state of the art.

Research efforts have been focused in two general directions[1]: incremental optimization of the already mature Li-ion technology (advanced Li-ion) or bold modifications of its core components (post Li-ion). The latter approach includes intensive work on switching to different mobile cations (for example, Na^+ or Mg^{2+}), utilizing metallic anodes and employing solid electrolytes that give rise to solid-state batteries. Such post Li-ion strategies are not mutually exclusive and can be combined to tailor the characteristics of the battery to the requirements of the application. Their combination, for instance, could include a metal-anode solid-state battery with considerable potential improvements in safety and lifetime, as well as higher energy and power densities[2].

Fast-ion conductors or solid electrolytes lie at the heart of the solid-state battery concept. Our aim in this Review is to discuss the current fundamental understanding of the material properties of inorganic solid electrolytes that are relevant to their integration in solid-state batteries, as shown in Fig. 1. We focus particularly on recent contributions to reflect the present trends, directions and challenges in the field.

Advantages of solid-state batteries

The main proposed benefit of solid-state batteries has been their increased safety, which stems from the absence of flammable liquid electrolytes typically employed in Li-ion cells. Detailed thermal and mechanical abuse investigations are still pending, but preliminary thermal analysis results are promising[3]. The inherent slower reactivity of solids compared with liquids also leads to expectations of longer device lifetimes for solid-state cells. This has been demonstrated for solid-state microbatteries operating for more than 10,000 cycles[4]; but the scalability of this attribute has yet to be proven. A multitude of aging effects in Li-ion batteries are linked to the liquid electrolyte and are not expected in solid-state devices, for example, transition metal dissolution. However, gas evolution from the cathode materials can also be encountered in solid-state cells leading to safety and aging issues[3,5]. Furthermore, other aging mechanisms, such as mechanical degradation, might be exacerbated exactly due to the solid nature of the cells.

Inorganic solid electrolytes could also support battery operation at low and high temperatures (for example, –50 to 200 °C or higher) in which conventional liquid electrolytes would freeze, boil or decompose. The low activation energies for fast-ion conduction help to reduce the variation of ionic conductivity with temperature ensuring reliable operation. Moreover, no bulk polarization is expected in solid materials, due to the immobility of the anionic framework, potentially leading to higher power capabilities[2,6]. Kato et al.[7] have reported extraordinarily fast cycling of solid-state cells, for example, 18 C at 100 °C corresponding to charge–discharge times of 3 min. Nevertheless, such current densities remain challenging for cells with practical energy densities[8]. Indeed, solid electrolytes are not impervious to polarization at their interfaces with electrodes, the effects of which should be carefully understood.

Adoption of solid-state technology could lead to significant increases in energy density, which is the quantity of energy stored per volume or mass of a device and constitutes a critical feature for any energy storage application. Notably, bipolar stacking of the anode of one cell and the cathode of the next cell on the same current collector could be implemented, as exemplified in Fig. 1, to produce higher-voltage individual cells[9] and thus reduce the packaging. Another promising prospect is the stabilization of next-generation electrodes, the utilization of which has been deemed problematic in liquid-based cells. These high-performance

[1]LRCS, UMR CNRS 7314, Université de Picardie Jules Verne, Amiens, France. [2]Department of Chemistry, University of Bath, Bath, UK. [3]ALISTORE European Research Institute, FR CNRS 3104, Amiens, France. [4]RS2E (Réseau Français sur le Stockage Electrochimique de l'Energie), FR CNRS 3459, Amiens, France. [5]Present address: Department of Materials Science and Engineering, The National University of Singapore, Singapore, Singapore.
*e-mail: theo.famprikis@u-picardie.fr; m.s.islam@bath.ac.uk; christian.masquelier@u-picardie.fr

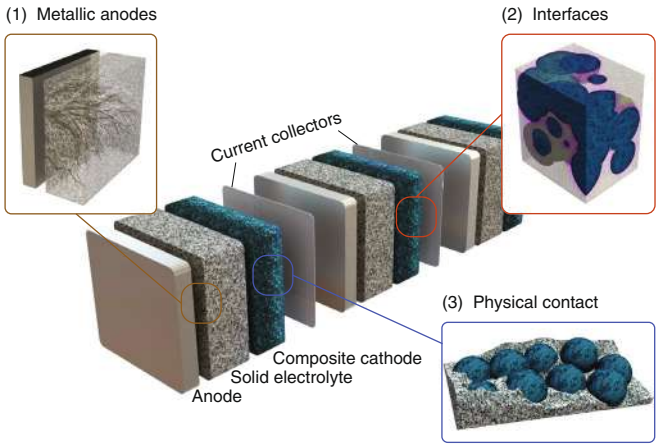

Fig. 1 | Schematic representation of a bipolar-stacked solid-state battery cell. Insets are magnified sections that highlight the three main challenges facing solid-state batteries with metal anodes: (1) inhomogeneous metal deposition, (2) formation of blocking interface and (3) contact loss on electrochemical cycling. The relative scale of the battery components is indicative of typical laboratory-scale cells. For commercial cells, inactive volume (solid electrolyte, current collectors, porosity) should be minimized and the electrodes should be balanced (chemically and mechanically[14]).

electrodes include metallic anodes, such as Li, Na and Mg, which could lead to the highest capacities and operating voltages in their batteries[2,10]. Similarly, high-voltage cathodes, can deliver more energy per ion transferred, but tend to cause oxidation of common liquid electrolytes. The use of metallic anodes and high-voltage cathodes with solid electrolytes has been demonstrated in solid-state microbatteries[4]; however, their applicability to large-scale systems remains to be proven.

Challenges facing solid-state electrolytes

In view of the advantages of solid-state batteries, intensive efforts have been dedicated to their development. Three main electrolyte-related challenges have been identified for solid-state battery devices[2], as shown schematically in Fig. 1.

Utilization of metal anodes is very problematic in liquid-based cells due to the inhomogeneous deposition of Li (or Na) as filament-like structures, commonly known as dendrites[11], which grow through the separator to the cathode causing short-circuit. It had been originally expected that solid electrolytes would be impervious to this dendrite-induced failure by virtue of their mechanical rigidity, but recent reports have demonstrated the ability of metallic Li to penetrate into solid materials[12]. Extensive efforts to fully understand the fundamental mechanism of inhomogeneous deposition of Li through solid electrolytes are underway.

A second challenge is stabilization of interfaces. The interfacial composition and structure between solid electrolytes and electrode materials often present major deviations from those of the bulk materials. The formation of ionically resistive or electron-conducting decomposition products have inhibited the performance of solid-state devices. Numerous experimental and computational techniques have been developed to probe the formation and behaviour of such interfaces. Elucidating the nature of interfaces will contribute to establishing a rational approach towards the combination of materials in the new generation of solid-state cells.

The third challenge is maintenance of physical contact. A prominent disadvantage of solid-state systems is the reliance of ionic diffusion on contact of solid particles. These point contacts are especially sensitive to stresses developed on electrochemical cycling in electrode materials[13], which can lead to the formation and propagation of cracks[14], as well as delamination of interfaces[15,16]. The development of effective strategies to alleviate the issue of physical contact is imperative in the engineering of solid-state batteries.

The solutions to these challenges hinge on our knowledge of the fundamental properties of solid electrolyte materials. Here, we review the current state-of-the-art understanding of inorganic solid electrolytes in the areas of multiscale ion transport, electrochemical stability and mechanics, and their reliance on the processing routes available.

Multiscale ion transport

The migration of ions in a solid-state battery is a multiscale process composed of mechanisms that manifest at different length scales, from the atomic scale up to the device scale, as shown in Fig. 2. Importantly, the final impedance of a device is a function of all these mechanisms. The techniques that can be used to probe ion conduction at varying scales are diverse and are often limited in their space or time resolution, making multi-technique approaches imperative for successful interpretation.

Atomic scale. At the atomic scale (Å), mobile cations (for example, Li^+, Na^+ or Mg^{2+}) diffuse in solids along favourable migration pathways and can be visualized as ion hops between ground-state stable sites and/or intermediate metastable sites of the framework constituted of anions (for example, O^{2-}, S^{2-} or polyanionic moieties). The sites and their energies are mainly defined by their local ion coordination, that is, bonding environment, which in crystalline compounds tends to be tetrahedral or octahedral. Consequently, the migration pathway of an ion in a material is a function of the availability and interconnectivity of different sites as defined by the arrangement of anions. For crystals, it had long been noticed that body-centred cubic anionic frameworks were common among the best ionic conductors (for example, α-AgI)[17]. Wang et al.[18] recently proposed that this framework allows direct hops between adjacent tetrahedral sites with low activation energy (E_a) and does not necessitate tetrahedral-octahedral hops with high E_a. Indeed, this body-centred cubic arrangement of anions is present in several fast ion conductors, such as $Li_{10}GeP_2S_{12}$ and $Li_7P_3S_{11}$ and provides a design criterion in the search for new materials.

In the crystalline case, cationic vacancies or interstitials are perceived as the mobile charged species. The three principal migration mechanisms shown in Fig. 3a are: (1) vacancy diffusion in which an ion migrates into a neighbouring vacant site, (2) direct interstitial mechanism between sites not fully occupied and (3) concerted or correlated interstitialcy (knock-on) mechanism, where the migrating interstitial ion displaces a neighbouring lattice ion into the adjacent site.

The mobility, u, of an ion in a solid electrolyte captures its ability to move through the solid lattice. The product of charge (q), concentration (n) and mobility of charge carriers in a solid then defines its ionic conductivity, σ, which is the key descriptor for ion transport (equation (1)). We note that typically, only a fraction of total ions in a solid is mobile but quantification of n (for example, ref. [19]) is not commonplace. Ion conduction is a thermally activated process described by a modified Arrhenius relationship:

$$\sigma = q\, n\, u = \sigma_0 T^m \mathrm{e}^{-E_a/k_B T} \quad (1)$$

with m typically equal to -1, k_B the Boltzmann constant, T the temperature and E_a a characteristic activation energy for ion conduction. E_a includes the energy needed to form the mobile defects (E_f) and the energy barrier for their migration (E_m), which corresponds to the highest energy along the conduction path, that is, the transition state for conduction, as shown in Fig. 3. For the simplest case of direct, uncorrelated hopping, the pre-factor, σ_0, the entropy of

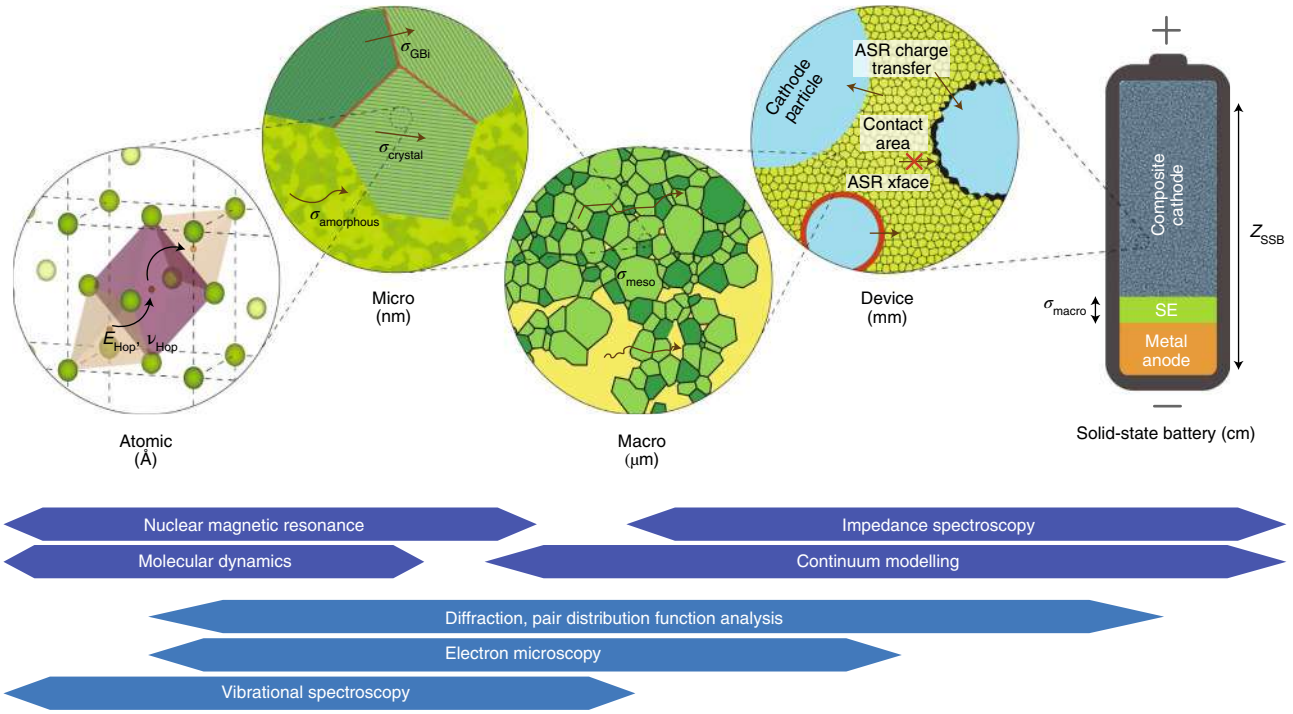

Fig. 2 | Multiscale ion transport and major associated techniques. Arrows denote the transport of mobile cations in the solid electrolyte (SE) framework (in green). The major descriptors relating to ion transport are highlighted at each length scale: energy (E_{Hop}) and frequency of hops (ν_{Hop}) at the atomic scale; the conductivities (σ_i) and area-specific resistances (ASR_i) of defining features at larger scales; culminating in total device impedance, Z_{SSB}. The techniques utilized to directly probe ion transport (that is, quantitatively determine the above descriptors; in dark blue) and complementary methods used to aid interpretation (in light blue) are placed in their associated length scales.

migration (ΔS_m), the jump distance (α_0) and the attempt frequency (ν_0), are related as follows:

$$\sigma_0 = z\frac{nq^2}{k_B}e^{\Delta S_m/k_B}\alpha_0^2\nu_0 \quad (2)$$

The geometric factor z (≤ 1) depends on the directionality of the conduction mechanism. 'Energy landscape' schematics are commonly used to visualize E_m, ν_0 and α_0, as well as the various conduction mechanisms, as shown in Fig. 3.

In the intrinsic regime, the concentration of mobile charged species, n, is temperature dependent and relates to the defect formation energy of vacancies and/or interstitials (E_f). Ion doping by substitution of aliovalent ions (that is, dopants with a different valence from the host ions) can also create charge-compensating vacancies or interstitials. For example, Si^{4+} dopants on the P^{5+} site in Na_3PS_4 create Na^+ interstitials[20], while Cl^- dopants on the S^{2-} site in the same material generate Na^+ vacancies[21]. In this extrinsic regime, the defect population is determined by the dopant concentration and in the case of both $Na_{3+x}Si_xP_{1-x}S_4$ (ref. [22]) and $Na_{3-x}PS_{4-x}Cl_x$ (ref. [23]) leads to significantly increased conductivities, in accordance with equation (2).

However, the effect of elemental substitutions is not limited to the concentration of mobile defects. For example, extensive cation mixing in the lithium superionic conductor (LISICON)-type $Li_{4\pm x}Si_{1-x}X_xO_4$ (X = P, Al and/or Ge) was shown to promote the change of the atomistic conduction mechanism to a 'superionic' one, attributed to a flattening of the energy landscape, thus enabling low migration energies[24,25]. Other authors have argued that increasing the mobile ion concentration above the number of available ground-state sites in materials, such as garnets and NASICONs (sodium superionic conductors), forces excess mobile ions into higher-energy (metastable) sites and enables concerted ion migration, that is, collective migration of multiple cations, akin to the intersticialcy mechanism shown in Fig. 3a, with reduced migration energy[26,27].

Anion frameworks that are mechanically softer, such as sulfides or selenides, have been thought to aid ion migration[28]. However, there are two competing effects arising from softer lattice phonons[29]: (1) the activation energy for conduction (E_a) decreases, aiding ion diffusion, but (2) lower lattice vibration frequencies simultaneously lead to lower hopping attempt frequencies, ν_0, and decreasing the migration entropy, ΔS_m (ref. [30]), thus promoting a decrease of the Arrhenius pre-factor (equation (2)). Recently, Kraft et al. demonstrated that the attempt frequency correlates closely to the Debye frequency derived from speed-of-sound measurements, which can act as a convenient descriptor for further investigations on ionic conductors[29]. Muy et al. also confirmed the correlation between the activation energy for conduction (E_a) and the phonon band centres using inelastic neutron scattering on a variety of oxide and sulfide LISICON materials[31].

Rotations of polyanionic moieties (for example, SO_4^{2-} and PO_4^{3-}) have been proposed to aid ionic conduction and have been referred to as the paddle-wheel effect[17]. Such explanations have recently resurfaced in light of computational results suggesting correlation between ionic conductivity and the rotational freedom of polyanions (typically tetrahedra including PS_4^{3-} (ref. [32]) or BH_4^- (ref. [33]), but also OH^- (ref. [34]) dipoles). Quasi-elastic neutron scattering experiments have attempted to provide direct evidence of paddle-wheel effects, most recently in $LiCB_{11}H_{12}$ and $NaCB_{11}H_{12}$, demonstrating a link between $CB_{11}H_{12}^-$ rotational mobility and Li^+ or Na^+ diffusivity[35,36].

Since the charge transfer in solid electrolytes is directly linked to mass transfer of the charged defects, it is often insightful to consider their diffusivity, D, linked to the conductivity by the well-known Nernst–Einstein relationship

$$D = \frac{u}{q}k_BT = \frac{\sigma}{nq^2}H_Rk_BT \quad (3)$$

where H_R is the Haven ratio, which is related to the factor z in equation (2), and depends on the specific atomic-scale diffusion

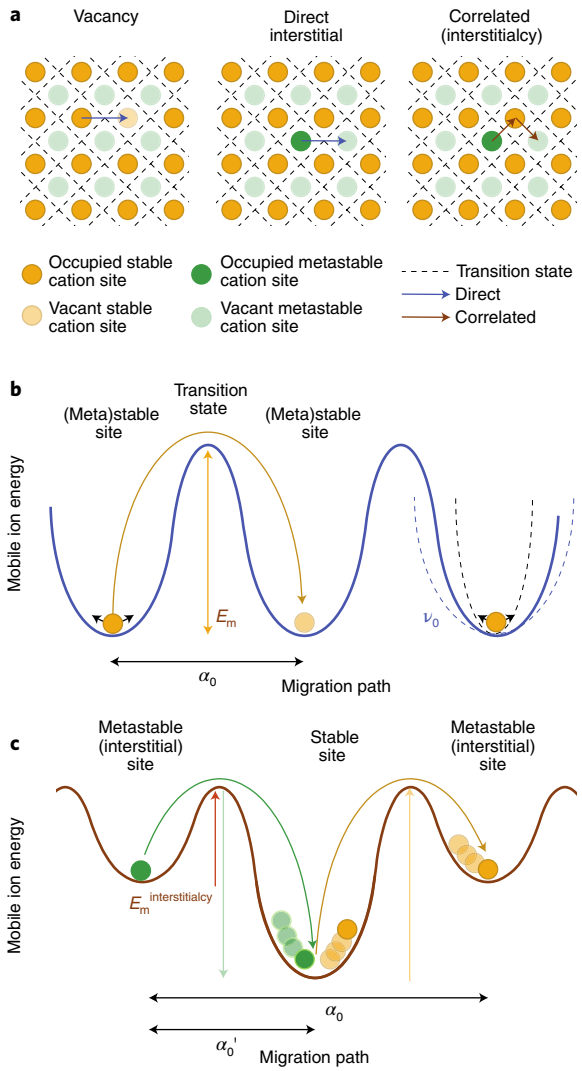

Fig. 3 | Cation migration mechanisms and associated energy profiles. **a**, The arrows indicate three typical migration mechanisms: vacancy, direct interstitial and correlated (interstitialcy) involving a single or multiple sites (blue and red, respectively). Circles represent cations in stable (green) and metastable (orange) sites of a model crystal lattice. Dotted lines represent the transition state for cation hopping as imposed by the anionic framework (not shown explicitly). **b**,**c**, The energy profiles associated with cation migration via direct vacancy or interstitial hopping (**b**) and correlated hopping (**c**) are shown with their associated hopping energies, E_m, hopping distances α_0 and hopping frequencies, ν_0.

mechanism. D is typically accessible by nuclear magnetic resonance (NMR) spectroscopy[37] and molecular dynamics simulations, from which equation (3) has been routinely applied to derive values of ionic conductivity[24,38]. Despite reasonable agreement between the different techniques (for example, ref. [24]), we note that (1) the different techniques probe ion transport at different scales (Fig. 2) and (2) there is recent debate about the validity of equation (3) in the case of solid electrolytes where the migration of multiple defects is highly correlated, the precise concentration of mobile charge carriers is unclear and/or in solid electrolytes that exhibit anisotropic migration pathways[39].

While crystalline materials have provided an excellent platform to develop our understanding of ion conduction, some of the most relevant solid electrolytes show partial or complete amorphous character. The lack of long-range periodicity in these materials implies the absence of regular coordination sites and symmetric long-range migration pathways. Despite diligent efforts, a unified theory for conduction in the amorphous state is not fully established[40,41]. Nevertheless, elements of the hopping theory can still be utilized, but require a statistical treatment, such as considering a distribution of activation energies for hops instead of a discreet one. Pair distribution function analysis of total scattering data[42] in combination with reverse Monte Carlo approaches, can provide direct visualization of the atomic arrangements and diffusion pathways in amorphous samples[43,44]. Such analyses, corroborated by NMR, vibrational and X-ray photoelectron (XPS) spectroscopies, may serve to establish the link between structural units (for example, the anion framework) and conductivity in glasses[45,46]. Due to the large system sizes required for satisfactory statistical analysis, direct probing of ion dynamics at the atomic scale by ab initio molecular dynamics calculations can be difficult[38]. Nevertheless, promising alternatives are being developed, including classical interatomic potentials derived from machine learning for amorphous Li_3PO_4 (ref. [47]).

Micro- and mesoscopic scales. Compositional or structural inhomogeneities manifesting at the nanometre to micrometre scales can often dominate the macroscopic ionic conductivity, either beneficially[48–50] or detrimentally[51,52]. The prime example of microstructural features are grain boundaries, surfaces of contact between crystallites of different orientation in polycrystalline samples, which can differ extensively from the bulk crystal in terms of structure and composition. Grain boundaries have been shown to increase the resistance for ion migration in most cases, making them undesirable in macroscopic samples. It has been proposed that positive space charging (anionic vacancies) can render grain boundaries repulsive for mobile cations[51] and that grain boundaries can act as sinks of ionically blocking impurities[53]. From an atomistic point of view, it has been shown that the percolation of mobile cations can be severely blocked by the distortions imposed by the misalignment of grains[52]. The magnitude of the effect depends on the material and seems to be negligible for sulfide solid electrolytes[54]. It is also conceivable that grain boundaries in certain materials could also aid conduction parallel to their surface by forming pathways of undercoordinated sites. In general, control over the concentration and atomistic nature of grain boundaries can lead to tuning of ionic conductivity[52,55] and, although sometimes tedious, the development of inventive techniques for their characterization (for example, ref. [54]) will be insightful.

There is growing interest in glass-ceramic ion conductors, which are materials that result from a controlled crystallization of an amorphous phase[56]. This is because in some materials, the glass-ceramic microstructure can result in stabilization of metastable crystal structures, such as $Li_7P_3S_{11}$ (refs. [45,57]) with an increase of ionic conductivity by several orders of magnitude. It has recently been shown that highly performing ionic conductors, previously thought to be completely amorphous, as determined by X-ray diffraction, might be composed of nanocrystallites embedded in an amorphous matrix, as demonstrated for 'glassy' Li_3PS_4 with high-resolution transmission electron microscopy[49]. Such nanocrystalline microstructures have been proposed to enchance conductivity by activation of surface conduction mechanisms in multiple materials, such as Li_3PS_4 (ref. [48]), and $LiBH_4$ (ref. [50]). Understanding of these synergistic effects of amorphous and crystalline phases constitutes an exciting avenue for further development.

Another source of resistance to ion transport for solid electrolytes and solid-state batteries is inadequate physical contact between solid particles. In polycrystalline materials and composite electrodes, the contact between solid particles must be maximized and maintained for efficient ionic conduction to take place. In contrast, the existence of porosity implies the occurrence of tortuous

paths for ion conduction and inhomogeneous current densities. These effects contribute to an increase of observable resistance to macroscopic ion transport. Therefore, the effective densification of polycrystalline solid electrolytes and composite electrodes becomes crucial to enhance ionic transport, but may represent a major challenge when the mechanical properties and the processability of solid electrolyte (and electrode) materials are taken into account. For both oxide[55] and sulfides[58], a decrease in porosity has been correlated with increased conductivity as a result of stronger grain–grain or particle–particle contact.

Macroscopic scale. The ionic conductivity of solid materials is typically measured on macroscopic samples, often pellets, through impedance spectroscopy measurements. Impedance spectra are sensitive to structural features in all preceding length scales and measure the total macroscopic ionic conductivity. Deconvoluting each component of the total macroscopic ionic conductivity, such as point contacts, grain boundaries, amorphous phases and impurities, requires fitting to abstract models often based on empirical hypotheses involving the observed capacitances. As a result, the reproducibility of impedance spectroscopy-derived conductivities (and associated activation energies) between research groups can vary within about an order of magnitude, as, for example, for the recently discovered $Na_{11}Sn_2PS_{12}$ (refs. [59,60]).

Much of the research effort in the past decade has been focused on maximizing the overall ionic conductivity of macroscopic solid electrolyte samples, σ_{macro}. This has led to macroscopic, ambient-temperature conductivity values, of the order of 10 mS cm^{-1} for Li^+ (ref. [7]), 1 mS cm^{-1} for Na^+ (refs. [59,60]) and 0.1 mS cm^{-1} for Mg^{2+} (ref. [61]). Notably, these values of ionic conductivity are directly contesting those of liquid electrolytes (~10 mS cm^{-1}) and numerous previous reviews have carefully discussed relevant trends of various material families[62,63].

Device scale. The critical impedance value Z_{device} is obtained at the device level, and includes contributions from materials other than the solid electrolyte, particularly, the conductivity of interphases that might form. Drawing a link between σ_{macro} and Z_{device} is not trivial, in that a straightforward combination of solid electrolytes with the highest ionic conductivity and high-performance electrodes does not necessarily lead to high-performance batteries. For example, limited performance was shown for Li_6PS_5Cl argyrodite electrolytes combined with the commercial electrodes $LiCoO_2$, $LiNi_{1/3}Co_{1/3}Mn_{1/3}O_2$ and $LiMn_2O_4$ (ref. [64]). The majority of solid electrolytes are unstable and decompose in contact with electrode materials[65]. The interphases formed are typically resistive to ion transport and represent one of the main roadblocks to ionic conduction[66,67]. As such, an electrolyte with much lower macroscopic conductivity can exhibit lower device impedance if it manifests more favourable compatibility with the electrodes[4].

In practice, the thickness, t, of planar conductive features, such as interfaces is often irrelevant or hard to determine experimentally, but can be assumed constant (in the case of passivated interphases). Rather than conductivity, it becomes more convenient to discuss impedence in terms of a thickness-independent area-specific resistance (ASR), equal to t/σ.

The contribution of the ASRs to the overall impedance for a given material pair then only depends on the area of ionic contact between the solid electrolyte and active material, typically quantified in terms of contact area per volume of composite[68]. It follows that ASR should be minimized and the contact area maximized. It is noted however, that this is the same contact area that is susceptible to resistive interface formation and degradation on cycling. The effect of such interphase resistances can range from dominating (kΩcm^2) to negligible[67,69–71]. For composite electrodes, the active area of ionic contact between electrolyte and active electrode material can be approximated electrochemically and is often much less than the total area of active material[72,73]. Special engineering must go into the 3D structure of composite electrodes with the goal of maximizing the coverage of electrodes by solid electrolytes[68]; in contrast to liquid electrolytes, which 'simply' wet the electrode particles.

Micro- and mesostructural parameters can once again dominate the overall ion transport at the device scale[74]. Similarly to the separator layer, porosity in the composite electrodes implies tortuous and/or blocked paths for ionic and electronic conduction and can severely limit the performance of the device[75]. For high energy density and to ensure sufficient electronic percolation, the volume fraction of solid electrolyte in the electrodes should be minimized to at least <50% (ref. [68]). However, lower solid electrolyte contents decrease the effective ionic conductivity of the composite electrode[75] and this fraction should remain >25% to avoid ionic percolation limitations[68]. Naturally the above thresholds are also a function of particle size (distribution) in the composites and smaller electrode (and electrolyte) particle sizes promote both lower electronic and ionic percolation thresholds, respectively, and high active area of ionic contact available to charge transfer[68,74,76]. In turn, charge-transfer resistances depend strongly on the electronic and ionic conductivity of the involved phases and consequently on cycling rate[74] and possibly induced space charging effects[77].

Any change in the chemical potential of the mobile species, such as at the interface between solid electrolyte and electrode, will generate a driving force for charge reorganization due to equilibration of the Fermi energies[78]. At thermodynamic equilibrium, the voltage versus Li/Li$^+$ is connected to the Li chemical potential μ_{Li} according to:

$$V = -\frac{\mu_{Li}}{qF} \tag{4}$$

where F is the Faraday constant. In the interfacial region, the μ_{Li} (voltage) undergoes a drastic variation (several mV nm^{-1}). The low voltage of the anode drives mobile cations into the electrolyte and vice versa for the cathode, inducing the depletion or accumulation of charge carriers and creating nanometre-length space-charged regions (Fig. 4)[6,77,78]. Such an effect might be exacerbated in solid-state batteries due to the inability of solid electrolytes to exhibit bulk polarization in contrast to liquids due to their lower permittivity[6].

Most importantly, this rearrangement of mobile species constitutes the first step towards possible decomposition of solid electrolytes. Understanding these decomposition reactions and employing strategies to increase the effective electrochemical stability of solid electrolytes are imperative for long-term stable operation and are central to the following section on electrochemical stability.

Electrochemical stability

Electrochemical reactions can be observed on contact at the interface of the solid electrolyte and electrode. The driving force for such reactions originates from the thermodynamics of mixing the compositions of the solid electrolyte and the electrode to create new stable phases, denoted the interphase, as shown in Fig. 5a. (The term interface refers generally to the area of contact between two phases, whereas the term interphase refers to the new phases that are formed at the interface due to electrochemical reactions.) We distinguish between pure redox decomposition of the electrolyte and chemical reactions between electrolyte and electrode.

Redox decomposition is characterized by the addition or extraction of electrons and/or mobile cations (Li^+, Na^+ or Mg^{2+}) in the solid electrolyte when paired with the electrodes. An example is the reaction of Li_3PS_4 in contact with Li metal[65,79–81]:

$$\begin{aligned} &2Li_3P^{V}S_4 + 2e^- + 2Li^+ \leftrightarrow Li_4P_2^{IV}S_6 + 2Li_2S \\ &\left(Li_4P_2^{IV}S_6 + 14e^- + 14Li^+ \rightarrow 2Li_3P + 6Li_2S\right) \end{aligned} \tag{5}$$

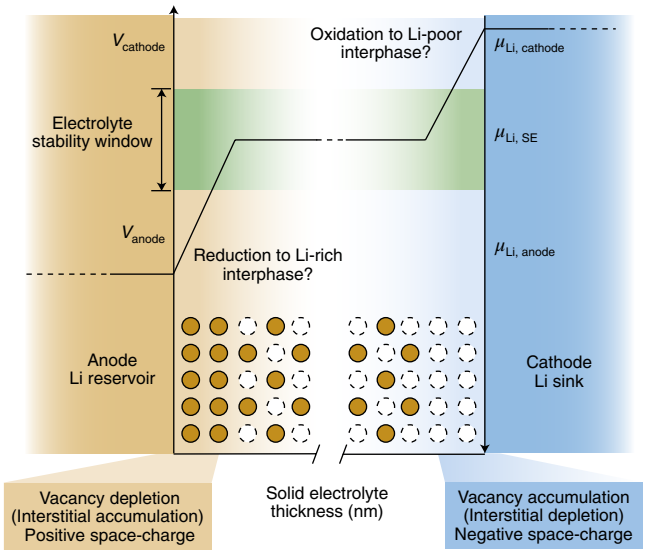

Fig. 4 | Evolution of chemical potential across the solid electrolyte in contact with an anode and a cathode. The *y* axes denote the voltage (*V*, increasing) and the chemical potential (μ, decreasing) (see equation (4)) of the mobile cation as a function of the solid electrolyte (SE) thickness on the *x* axis. The evolution of the chemical potential leads to a concentration of the mobile cation close to the anode and dilution close to the cathode. These concentration gradients can directly lead to decomposition of the solid electrolyte and/or reaction with the electrodes. This phenomenon exemplified here for Li can also apply to Na and Mg.

Such reactions can be partially reversible[79], as exemplified by a solid-state battery made from a single material, $Li_{10}GeP_2S_{12}$, oxidized and reduced reversibly[82].

In contrast, chemical reactions involve the formation of new phases in the combined compositional space of the electrolyte and cathode materials. For example, at the interface of Na_3PS_4 and layered $NaMO_2$ (M = Co, Ni, Mn or Cr), the O^{2-}–S^{2-} displacement reaction is predicted[83,84]:

$$Na_3PS_4 + 2NaMO_2 \rightarrow Na_3PO_4 + 2NaMS_2 \quad (6)$$

Redox and chemical reactions can happen in sequence or simultaneously, together dictating the electrochemical stability of the solid electrolyte. The extent of such reactions depends highly on the power applied and the state of charge of the battery. For example, at the interface of Li_3PS_4 and $LiCoO_2$, the following reaction is predicted[65]:

$$2Li_3PS_4 + 3LiCo^{III}O_2 \rightarrow Co^{II}(PO_3)_2 + 2Co^{IV}S_2 + 4S^{\emptyset} + 9e^- + 9Li^+ \quad (7)$$

In practice, rather than formation of distinct stoichiometric phases, intermixing might also occur at the interface. Such intermixing is the case of equation (7), where the interphase was composed of nanocrystals rich in Co and S as well as extensive P, Co, O and S interdiffusion between electrolyte and electrode, as characterized by transmission electron microscopy[66].

The stability window of an electrolyte is the voltage range that it can sustain without redox decomposition, as indicated schematically in Fig. 4. Thermodynamically, the stability windows can be defined by considering the free energy of the decomposition reactions as a function of the voltage. Richards et al. developed a methodology to calculate the energies of such reactions for a multitude of Li solid electrolytes by utilizing μ_{Li} as a proxy for the voltage (equation (4))[65], and other researchers have expanded this for Na (ref. [84]) and Mg (ref. [85]) creating effective libraries of stability windows. In practice, such computed stability windows may be extended due to stabilizing kinetic effects. A certain 'overpotential' beyond the thermodynamic stability limit is often required to drive the atomic rearrangements associated with decomposition, for example, about ±0.5 V in the case of Na_3PS_4 (ref. [83]). The magnitude of this required overpotential could be linked to the mobility of charged species in the electrolyte[86], which would explain the trend for the most conductive electrolytes to decompose most easily in contact with electrodes.

The high-voltage oxidation stability of solid electrolytes is largely set by the anion framework and specifically its propensity to give up electrons, typically limited by the anion with the lowest ionization potential following the order $N^{3-} < P^{3-} < H^- << S^{2-} < I^- < O^{2-} < Br^- < Cl^- << F^-$ (ref. [65]). Inversely, the stability against reduction is set by the propensity of the solid electrolyte to accept electrons, accounted by the electron affinity of the (non-mobile) cations. We note that the electron affinity can be affected by the specific structure and bonding characteristics. For example, a phosphorus atom will be reduced more easily if weakly bonded to sulfur atoms compared with when strongly bonded to oxygen species, as exemplified by the increased stability of Li_3PO_4 compared with Li_3PS_4 (ref. [65]). Indeed, the stability against reduction has been experimentally correlated with bond stiffness of polyanion units[31] for a variety of LISICON-type materials. The stability of solid electrolytes of analogous composition against reduction might be better against Na metal compared with Li due to their difference in absolute potential, as suggested for example by the stability of $NaBH_4$ versus Na^0 in contrast to the instability of $LiBH_4$ versus Li^0 (ref. [87]).

It is important to note that electrochemical reactions at the solid electrolyte/electrode interface do not necessarily preclude battery functionality. Given that reactivity is favoured, the kinetics and consequently the extent of reaction are governed by the interfacial transport properties. As evident from equations (5) and (7), the electrochemical reactions at the electrodes typically involve cation (Li^+, Na^+ or Mg^{2+}) and electron mobility. If either is impeded, the reaction is blocked and the interface becomes kinetically stabilized. However, for the battery to function, mobile cations must transverse the interface. As such, the ideal interphase for a battery will be a good ionic conductor and an excellent electronic insulator. Such a scenario will lead to an interphase of finite thickness, stable against further electrochemical decomposition with a constant impedance contribution to the full cell. In the worst case, an interphase that is sufficiently conducting for electrons and mobile cations, denoted as a mixed-conducting interphase, can sustain extensive reactions, leading to an ever-growing thickness[71], unmanageable resistance and short-circuit in the case of metallic anodes. Solid electrolytes containing metallic elements are especially prone to form such interphases at low voltages, due to their tendency to reduction, for example, Ti in NASICONs and perovskites[80,88] or Ge in NASICONs, LISICONs and $Li_{10}GeP_2S_{12}$ (refs. [69,89,90]).

In Fig. 5b, we have identified three types of functional interfaces that can serve to operate solid-state batteries: (1) intrinsically stable, (2) kinetically stabilized and (3) artificially protected.

Intrinsic stability relates to the case of no reactivity between the two materials. This is an ideal case and almost no such interfaces are known with metallic electrodes with a notable exception of Na-β-Al_2O_3 versus Na metal[91]. A debated case is that of doped $Li_7La_3Zr_2O_{12}$ garnet, which becomes slightly lithiated on contact with Li metal. This lithiation causes a phase transition from the cubic to the tetragonal phase[92,93]. The macroscopic ionic conductivity of the tetragonal phase is lower, but it barely limits conduction as a nanometric film, constituting an ideal interphase[92]. It is worth noting that theoretical investigations reveal instead a slight thermodynamic instability of $Li_7La_3Zr_2O_{12}$, albeit at very low potentials

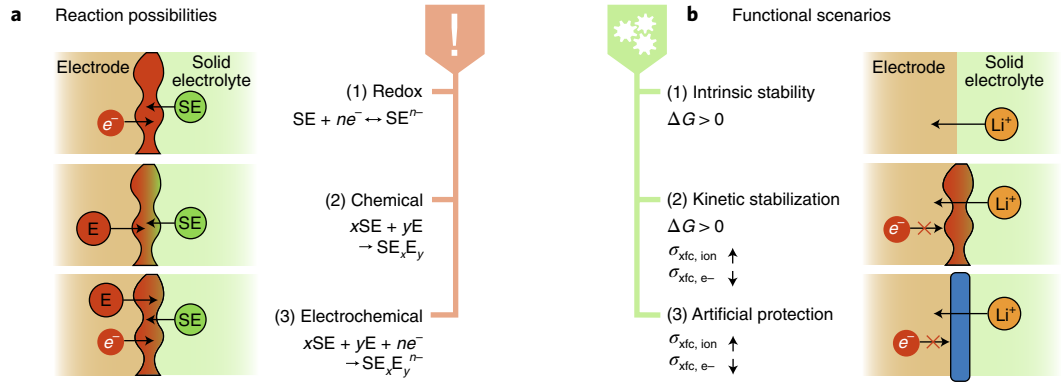

Fig. 5 | Reaction possibilities and functional scenarios for solid electrolyte/electrode interfaces in solid-state batteries. a,**b**, Illustration of the parasitic (1) redox, (2) chemical and (3) electrochemical reactions that can take place depending on their respective free energy, ΔG (**a**), imposing the need for interface (xfc) engineering of functional batteries through (1) intrinsic stability, (2) kinetically stabilized decomposition and/or (3) artificial protection strategies (**b**). Effective interfaces will allow Li^+ diffusion and prevent electrons or other atoms/ions from interdiffusing. SE and E denote atomic species in the solid electrolyte and electrode materials, respectively. *x*, *y* and *n* are stoichiometric coefficients and *n* can be positive or negative (reduction or oxidation, respectively).

(0.05 V versus Li^0) and with low reaction energies (20 meV per atom)[65,80]. As such the observed stability of garnet electrolytes against Li^0 is likely the result of kinetic stabilization.

Lithium phosphate oxynitride (LiPON) constitutes an excellent example of kinetic interface stabilization[94]. LiPON decomposes into Li_3PO_4 and Li_3N (among others) to form a functional interphase that is nanometrically thin, electrochemically stable and ionically conductive[65,94] rendering its decomposition negligible with respect to the electrochemical performance of the battery. Computationally predicted decomposition reactions of solid electrolyte materials in the presence of electrodes[65,80,84] can be directly used to assess the compatibility between solid electrolytes and electrodes as well as to design novel solid electrolytes with engineered decomposition. The rational design of new solid electrolytes could mimic the practice of additive inclusion in liquid electrolytes to stabilize the solid electrolyte interphase.

Artificial protection involves the inclusion of a preformed coating layer as a buffer material between the solid electrolyte and the electrode, with the goal of modifying the effective stability window of the solid electrolyte. Coating materials, typically acidic oxides (for example, $Li_4Ti_5O_{12}$ (ref. [95]), $LiNb_{1-x}Ta_xO_3$ (refs. [7,70]) or $Li_{3-x}B_{1-x}C_xO_3$ (ref. [96])) have become commonplace to protect solid electrolytes, mostly sulfides, from oxidation. The coatings are expected to smooth the voltage drop at the interface by providing an environment where the Li potential is intermediate between that of the solid electrolyte and the cathode materials (see Fig. 4). Some researchers maintain that the reduction in resistance is linked to a mitigation of space charging[77], but others propose that the critical action of these coatings is the insulation of the electrolyte/electrode interface against diffusion of electrons and non-Li atomic species[66,78]. Artificial protection strategies are also attempted on the anode side, especially for Li metal, but analogous work on Na- and Mg-metal anodes is still lacking.

Apart from reactions with the electrode materials, redox decomposition can also occur if the electrolyte is placed in contact with the electronic percolation network, such as any conductive additive or the current collectors themselves[83,97]. Thus, coating strategies might also have to be extended to additives and current collectors[97], or applied to the electrolyte particles instead. Another viable artificial protection strategy is the dual-electrolyte concept, where one solid electrolyte with high stability against reduction is in contact with the anode and another solid electrolyte stable against oxidation is placed against the cathode[7,98].

Ideal solid electrolyte/electrode interphases are nanometrically thin and 'buried' within the bulk of the composite electrode and represent only a very small fraction of the mass and volume of the battery. As such, their direct characterization is not straightforward. Electrochemical investigations can evaluate the effect of interphases on battery performance but cannot alone describe their underlying chemical nature. The importance of solid electrolyte/electrode interphases has ignited the development of numerous innovative techniques and experimental setups for their study, as summarized in Table 1.

Given the minimal thickness of the interphases, techniques with nanometric resolution provide distinct advantages to their understanding. Ex situ XPS has been successfully implemented in the post mortem analysis of buried interphases of Li_6PS_5Cl against multiple cathode materials[64]. Another approach involves taking in situ XPS measurements with the synchronous deposition of Li or Na to mimic the effect of lithiation/sodiation on contact of various electrolytes with the respective metals[94]. Other novel approaches include 2D exchange NMR experiments, which have helped to rationalize the observed rise of impedance in the Li_6PS_5Br/Li_2S interface on cycling[67]. Exciting avenues also include the development of in situ high-resolution transmission electron microscopy experiments to track the atomic rearrangements at the interface and elucidate their effects[92].

Another approach to study interfaces is by artificially promoting interfacial reactions. This can be achieved by preparing solid electrolyte/carbon composites acting as active electrodes and cycling them against the respective metal[83,99]. Mixing the solid electrolyte with carbon improves the electronic contacts, and eases the (de) intercalation of the mobile cations into and from the solid electrolyte on its reduction or oxidation[97]. As such, the interphase is formed at a much larger scale, and is thus accessible by more traditional bulk characterization methods (for example, diffraction)[83,99]. Alternatively, the identified decomposition products can be directly synthesized in bulk to study their relevant electrical and structural properties[100–102]. The disadvantage of these (ex situ) strategies is that spatial information regarding the size and morphology of the real interphase and specific resistances is lost.

In parallel, computational methods based on density functional theory can access thermodynamic quantities that compare directly with experiments, such as electrochemical stability windows[65,80] and chemical reactivity with specific electrodes[65,83,103]. However, two main limitations of computational methods can be identified: (1)

Table 1 | Experimental and computational techniques that have been employed to characterize solid electrolyte/electrode interfaces for solid-state batteries

	Technique (sub-techniques)	Observables/descriptors	Operando[a]	Sub-micron spatial resolution[b]	Representative examples
Electrochemistry	Impedance spectroscopy	Macroscopic resistances, capacitances, permittivity	X		Refs. 69,70,95
	Electrochemical (de-) lithiation/sodiation	Effective stability window			Refs. 83,99
	Full-cell cycling	Capacity fade, overpotential	X		Refs. 7,15
Spectroscopy	Nuclear magnetic resonance spectroscopy (pulse field gradient, 2D correlations)	Local structure, diffusivity and activation energy, charge transfer	X		Refs. 67,129
	X-ray photoelectron spectroscopy	Composition, local structure, oxidation states		X	Refs. 64,88,94,130
	X-ray absorption spectroscopy	Local structure, oxidation states		X	Refs. 101,131
	Raman spectroscopy	Local structure	X	X	Refs. 79,93
	Time-of-flight secondary ion mass spectrometry	3D composition		X	Refs. 132,133
Microscopy and Imaging	Scanning electron microscopy (energy dispersive spectroscopy, Auger spectroscopy)	2D microstructure, 2D composition		X	Refs. 15,64
	Transmission electron microscopy (electron diffraction, electron loss- and energy dispersive spectroscopy)	Atomic-scale structure, 2D composition, oxidation states		X	Refs. 66,92,134
	Neutron depth profiling	3D composition	X		Refs. 135,136
	X-ray tomography	3D microstructure	X		Refs. 70,137
Computation	Phase diagrams from first principles	Composition, thermodynamic stability window	NA		Refs. 65,80
	Molecular dynamics	Atomic-scale structure, reaction mechanism, diffusivity	NA	X	Refs. 84,138

The pertinent descriptors of interface performance that can be extracted from each technique (and sub-techniques) are listed along with representative examples from recent literature. [a]Allowing for probing of the interface in a working complete solid-state battery cell. [b]Allowing for spatial resolution at the 1–100 nm scale, typically required to spatially identify interphases.

the construction of phase diagrams depends on previous knowledge of the stable crystalline phases and (2) stabilizing kinetic effects are not captured explicitly.

The formation of interphases that might arise from possible electrochemical reactions involves atomic rearrangements and volume changes compared with pristine materials[84]. Changes of the chemical environment and strain evolution can affect the connectivity and contact between different phases and are therefore the origin of the challenge in maintaining physical contact, explored in the following mechanics section.

Mechanics

The mechanical properties of the solid electrolyte and associated interphases can affect the microstructural evolution of the battery and consequently its performance. Specifically, loss of contact, fracture and/or inhomogeneous electrodeposition (Box 1) can be catastrophic and all depend on the response of the solid electrolyte matrix to the developed stresses. However, the relationship between the mechanical properties of solid electrolytes and the performance of the solid-state battery is still poorly understood.

The role of external pressure on the operation of solid-state batteries has been highlighted previously[2] and specialized pressure setups are routinely used to effectively operate solid-state batteries at the lab scale[97,104]. Zhang et al. have observed a significant evolution of cyclic stress together with the solid-state battery operation[13]. It is crucial to consider the solid-state battery as a solid composite and treat its micromechanics[105], including its resilience to form cracks and the delamination of interfaces, as depicted in Fig. 6.

The tendency of the surfaces of two materials to keep together (or inversely the resistance to delaminate) is described by surface adhesion. It is a prime example of the electrochemomechanical coupling[105] that is crucial in solid-state batteries and necessitates multidisciplinary understanding of the contributions from: (1) the chemical interfacial energy, γ_{xfc}, corresponding to the difference in bonding and coordination at the interface compared with the bulk, (2) mechanical strain originating from lattice misfit between the contacted phases and (3) electrical attraction due to charge reorganization at the interface (shown in Fig. 4).

In the case of electrolyte decomposition in the presence of electrode materials, it remains challenging to identify the components participating in the adhesion of surfaces, and computational techniques may become insightful. The importance of adhesion has been qualitatively illustrated for the metal electrode/solid electrolyte interface by contact angle measurements of the liquid metal on the solid electrolyte, with treatments that improve the 'wettability' of the solid electrolyte correlating to lower interfacial resistance[106], probably due to vastly increased surface contact area. Wang et al. demonstrated the direct correlation between the adhesion strength, σ_{adh}, (pressure needed to delaminate) of a $Li/Li_7La_3Zr_2O_{12}$ interface to its interfacial resistance, thus showing the direct link between mechanical strength and effective ionic transport across interfaces[107].

The stress developed as a result of electrochemical reactions at the electrodes is termed electrochemical strain, $\varepsilon_{electrochemical}$, or electrochemical shock. As the mobile ion is reversibly inserted in the electrode materials, they undergo cyclical expansions and contractions. This phenomenon can result in localized stresses with

Box 1 | Interfacial and electrodeposition issues for metal anodes in solid-state batteries

There are two main interlinked issues hindering the application of metallic anodes (Li^0, Na^0 and Mg^0) in batteries: (1) their reducing nature that leads to reaction with the electrolyte, which increases resistance during electrochemical cycling and (2) their tendency for inhomogeneous electrodeposition during charging that ultimately leads to device failure by short-circuit. For solid-state batteries to supersede conventional liquid cells in terms of energy density, they have to feature a metallic anode[2]. Despite expectations to the contrary, solid-state systems are also prone to short-circuit by electrodeposition, which has long been observed for Na in Na-β-Al_2O_3 (ref. [140]) (and Ag in AgI and $RbAg_4I_5$ (ref. [141])). Recent experiments also confirm the problematic growth of Li through a range of solid electrolytes[12]. To curb these issues, alternative anodes, such as Li–In alloys, $Li_4Ti_5O_{12}$ (ref. [13]) and Na–Sn alloys[83] are typically utilized in current solid-state systems.

The manifestation of plating instabilities is intimately linked to the rate of electrodeposition with a critical current density typically utilized as the most accessible descriptor of resistance to this failure mechanism. In most Li-based inorganic solid electrolytes, the critical current density never surpasses 0.3 mA cm^{-2} (of real interfacial area) at room temperature, whereas for competitive Li metal batteries the target is 3–10 mA cm^{-2} (ref. [10]). Additionally, factors including the (area specific) resistance of the Li/solid electrolyte interface[106,142], temperature[143], electronic conductivity[137], microstructure and surface flaws[12] have been shown to affect the anomalous electrodeposition of Li in solid electrolytes. It is becoming clear that there are distinct mechanistic differences from the growth of dendrites in liquid electrolytes[10]. Solid-state setups often operate under applied pressure and are subjected to additional stresses developed during cycling. The metallic anode is thus under compressive stress of the order of megapascals, thus exceeding the yield strength of alkali metals (for example, ~0.8 MPa for Li (ref. [144])). In the case of solid polymer electrolytes, a high shear modulus may promote stable electrodeposition[145]. However, this criterion has been shown not to apply for inorganic solid electrolytes both theoretically[146] and by demonstrations of metallic Li growth through various materials[12], from soft thiophosphate glasses ($E \approx 20$ GPa and $G \approx 7$ GPa (ref. [108])) to stiff monocrystalline oxide garnets ($E \approx 150$ GPa and $G \approx 60$ GPa (ref. [147])).

The exact failure mechanism related to problematic electrodeposition of Li in solid electrolytes is not yet fully understood. Most recent studies support a mechanism that proceeds in the following steps: (1) Li tends to nucleate preferentially at grain boundaries, and/or voids. This is typically ascribed to inhomogeneities in the Li/solid electrolyte interface causing current hotspots (panel **a** in figure). This can be linked to the fabrication of the interface, including roughness, surface flaws, low adhesion or interphase formation and/or to inhomogeneous stripping during discharge. The current density concentrates at the hotspots with the consequent development of highly localized pressure and overpotentials[143]. The molar volume of Li is much higher in its metallic form than in any inorganic solid electrolyte[148] by a factor of ~10, causing extreme localized expansion and placing the solid electrolyte under stress. (2) Cracks propagate through grains, grain boundaries and/or voids and Li deposits inside them, eventually short-circuiting the cell[149] (panel **b** in figure). This electrodeposition-induced mechanical failure is counterintuitive, given that metallic anodes typically have yield strengths that are orders of magnitude lower than those of the solid electrolytes[150]. Once the cell is short-circuited, the mode of charge transfer switches to electronic, which has been reported to cause melting of Li via Joule heating[150]. Liquid Li tends to flow out from existing cracks and temporarily interrupt the short-circuit, therefore explaining the erratic voltage oscillations commonly observed in electroplating experiments[149,150]. Recently, it has also been proposed that electrons could penetrate the bulk of the solid electrolyte and cause direct nucleation of metallic Li away from the anode[137].

Based on the above description, several design principles for the stabilization of metal electrodeposition through solid electrolytes have been proposed. With respect to the Li/solid electrolyte interface, surface treatments that improve the adhesion of Li to solid electrolytes, quantified through wettability, have been successfully implemented to lower the interfacial resistance and thus increase the critical current density[142]. In the same vein, mechanical polishing[143] and coating thin films of buffer layers[106] can also promote the adhesion and homogeneity of the interface. Alternatively, designing electrolytes with respect to their decomposition can also lead to stable, ionically conductive and electronically blocking interphases[151]. Microstructuring electrodes to increase the real surface area helps to achieve higher critical current densities per footprint area[120]. It has also been argued that, in contrast to polymer electrolytes, inorganic solid electrolytes (or interphases) with lower shear modulus (for example, $LiBH_4$ with $G \approx 4$ GPa (ref. [148])) would be advantageous in maintaining homogeneous electrodeposition[146]. With respect to crack propagation, mechanical considerations would dictate the use of solid electrolytes with high fracture toughness by carefully controlling the microstructure, that is, grain size[55], porosity, pre-existing cracks[12] and pore connectivity[138]. In parallel, it was recently highlighted that more caution is warranted to minimize electronic conductivity of solid electrolytes as the key to stable metallic electrodeposition[137]. In the absence of a complete fundamental description of the anomalies of metal deposition through solid electrolytes, it is currently unclear which of the aforementioned factors is the most crucial for stable electrodeposition of Li, Na and/or Mg.

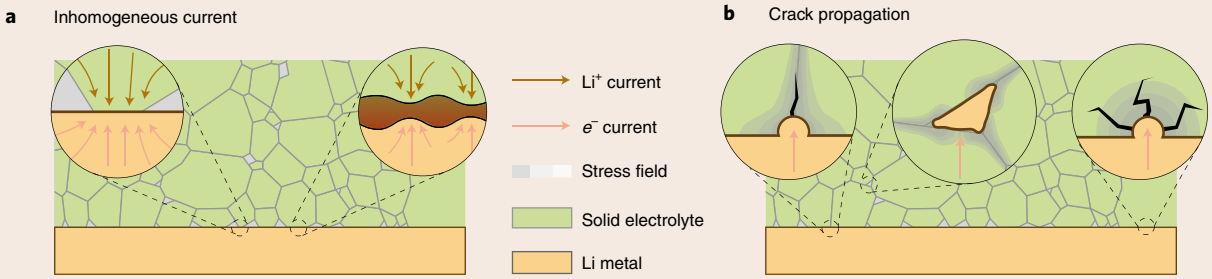

Inhomogeneous Li deposition through solid electrolytes. a, Imperfect contact and interphase formation (brown) cause current hotspots. **b**, Preferential Li deposition in grain boundaries, voids and/or within grains creates localized stress resulting in fracture. Li could be deposited directly in the bulk of solid electrolyte through electronic leakage if $\sigma_{el} \neq 0$.

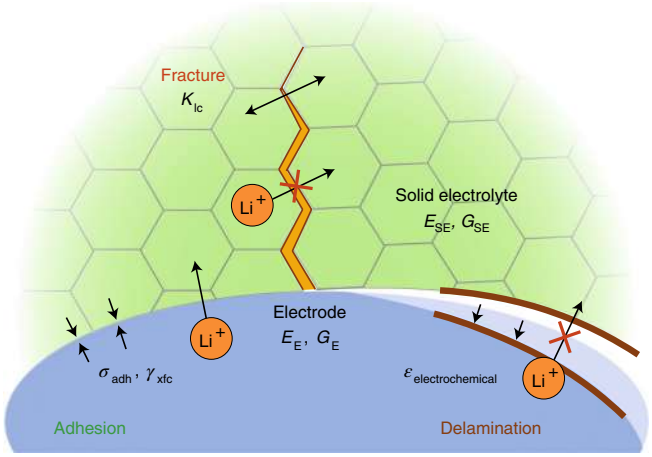

Fig. 6 | Mechanical degradation of a solid-state battery. The mechanical properties (Young's and shear moduli, *E* and *G*, respectively, fracture toughness K_{Ic}) of the solid electrolyte (SE) and electrode (E) dictate the response of the system to the strain ($\varepsilon_{electrochemical}$) during cycling. The adhesion of different solid phases in the composite can be quantified through the adhesion strength σ_{adh} and interfacial energy γ_{xfc}.

detrimental consequences, such as the formation of fractures and their propagation, delamination of interfaces and/or loss of contact between particles, as illustrated in Fig. 6. In such cases, voids are created adding up to the inactive volume of the battery, with direct consequences on performance. This phenomenon is in stark contrast to liquid-based systems where electrochemical strain results in hydrostatic pressure, which can be dissipated homogeneously, forcing the electrolyte to permeate any created voids and maintaining ionic contact. Furthermore, the negative and positive electrodes typically present unequal electrochemical strain, resulting in macroscopic pressure evolution on the device scale[14]. The magnitude of electrochemical strain depends largely on the electrode material used and can be negated by utilizing 'zero strain' electrodes, such as $Li_4Ti_5O_{12}$ (ref. [13]).

Material deformation under stress, including electrochemical shock, is generally described by the Young's (*E*) and shear (*G*) elastic moduli. It has been proposed that soft materials with low moduli, such as sulfides, would be ideal as solid electrolytes, accommodating applied stresses imposed by the electrodes during reversible ion intercalation. However, it has been demonstrated that such soft materials (for example, lithium thiophosphate glasses), remain brittle and prone to fracture on stress[108].

The resistance of solid materials to crack propagation is quantified by fracture toughness, K_{Ic}, which is emerging as a determining factor for charting the performance of solid-state batteries. Bucci et al. modelled the effects of cycling-induced fracture in a solid-state battery, namely increased impedance and capacity loss[109]. They proposed that high fracture toughness, typically exhibited by dense oxides, is beneficial to avoid the creation and propagation of fractures on electrochemical shock. Unlike the elastic moduli, fracture toughness is heavily dependent on microstructural parameters, such as densification, grain size, impurities and the occurrence of pre-existing cracks and porosity.

Despite the dependence of solid-state battery performance on mechanical properties, such characterization of solid electrolyte materials is not commonplace. Density functional theory calculations can provide estimations for the elastic moduli of pristine materials, whose atomic structures are known[110]. However, the fracture toughness greatly depends on the microstructure and will need to be determined experimentally[55]. The microstructure is a function of the processing route used for the synthesis of the solid electrolyte material and its integration in a solid-state battery, which is the subject of the following section on processing.

Processing routes

The choice of processing route directly controls the electrical, chemical and mechanical properties of materials and devices, and also determines their potential for scale-up. A solid electrolyte needs to be first synthesized from commercially available reagents, densified into a thin format to minimize ohmic resistance, and finally integrated into a solid-state battery through intimate mixing with the electrode materials, as presented in Fig. 7.

Synthesis. The most direct route to synthesize solid inorganic materials has been solid-state synthesis, meaning the 'shake and bake' mixing and annealing of dry powders. Although this strategy has proven successful in laboratories, solid-state routes often require high temperature, and consequently large energy consumption. In addition, the evaporation of volatile components (for example, Li_2O or Li_2S/S) complicates the accurate control of composition and often necessitates the use of additional sacrificial reagents, for example, refs. [29,55]. Furthermore, the increased temperature often leads to reactivity with the reaction vessel[111,112].

Soft chemistry involves wet processing of reagents in the presence of a liquid solvent; initially utilized as a way to control the microstructure of oxide solid electrolytes in conjunction with consequent high-temperature annealing. Recently, soft chemical approaches have been emerging as a standalone way to produce sulfide solid electrolytes at lower temperatures[48,56]. The lower energy requirement is an advantage for scalability and, depending on the solvent, such routes can be safe and sustainable. Nevertheless, careful manipulation and recycling of the solvent would be required. A high control over the purity and reproducibility can be ensured and soft chemistry methods have been employed to create completely new microstructures of known solid electrolytes with improved ionic transport[48,56].

Another successful approach in producing amorphous and glass-ceramic materials with superior properties is mechanochemical synthesis (typically ball milling) that relies on the high energy impact between solid particles[57]. Mechanochemical routes can sustain reactions at low temperatures, such as in the case of Li_6PS_5Cl (ref. [113]) or cause nucleation of metastable phases, such as for the cubic-Na_3PS_4 (ref. [114]). Although highly successful and practical on the lab scale, correlations between synthesis parameters and resulting products still remain empirical. Even though ball milling is already used industrially, its scalability with respect to safety and energy consumption remains debated. The main concerns originate from the sensitivity of resulting solid electrolytes to the mechanochemical parameters, such as weight ratios, media and speeds for ball milling and consequently limited reproducibility.

Overall, there is an empirical link between high ionic conductivity and metastability as quantified by positive calculated formation energies and challenging synthesis, for example, for $Li_{10}GeP_2S_{12}$ and its silicon analogue $Li_{11}Si_2PS_{12}$ (ref. [115]). High Li mobility often seems to come at the expense of stability. Nevertheless, all three main synthesis routes (solid-state, soft chemistry and mechanochemical) can potentially access such 'metastable' phases. In particular, solid-state routes can include a quenching step during which a high-temperature atomic configuration is 'frozen'. In mechanochemical routes, the high kinetic energy imparted on impact is quickly dissipated by the particles, which intrinsically mimics the conditions of quenching. Finally, solution methods offer considerable control over the particle morphology in the form of solvent–product interactions and can bring surface effects into play to similarly produce metastable phases[48].

Densification. Solid electrolyte powders, regardless of the synthesis method, need to be further processed into high-aspect-ratio membranes or pellets. High densification can be achieved through firing of green bodies (sintering) and cold or hot pressing of dry powders,

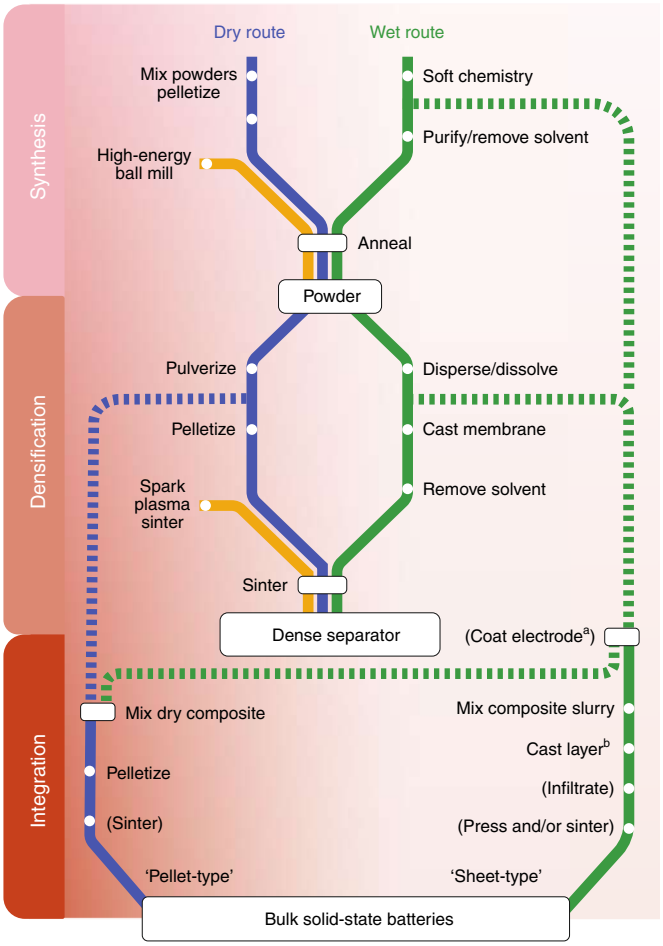

Fig. 7 | Simplified flowchart of available methods for the processing of solid electrolytes for solid-state batteries. From powder reagents to solid-state batteries, the solid electrolyte needs to be synthesized, densified and integrated into the device. These steps can utilize interchangeably either dry (blue) and/or wet (green) processing approaches. Auxiliary methods (yellow) such as mechanochemistry and spark-plasma sintering can also be utilized in specific parts of the process flow. [a]For example, sol-gel[70], spray drying[95], dip coating[122] and so on. [b]For example, tape casting, screen printing and so on[139].

to achieve the desired microstructure[55,116]. Softer materials such as sulfides and borohydrides might have a relative advantage against the typically refractory oxides due to their ability to be densified at low (even ambient) temperatures. The method of reference is spark plasma sintering, which enables precise control of the microstructure allowing for model experiments to probe its effects on ion transport[51,117]. However, such processing is currently prohibitively costly, limiting its utilization to research and niche high-performance applications.

Integration. In terms of complete solid-state battery integration, thin-film methods are the only industrialized route for manufacturing solid-state microbatteries[4]. Although thin-film methods boast great advantages in terms of minimal achievable thicknesses, high densification and excellent solid–solid contacts, their scalability for bulk solid-state batteries remains doubtful due to the costs involved. Fabrication of solid-state batteries by cold-pressing of dry components has been most popular at the lab scale but its applicability for scale up and hard oxide solid electrolytes is limited[118].

As outlined in the ion transport section, designing the 3D electrode geometry is key to maximizing the solid electrolyte/electrode interfacial area of ionic contact and thus minimizing the overall resistance of solid-state cells. Mesostructured and interdigitated designs have been explored for decades for microbatteries[119]. For bulk systems, numerous approaches are now being explored, for example, fabricating porous, 'trilayer' solid electrolyte frameworks using sacrificial porogens[118,120] or simply utilizing smaller cathode particles[76,121]. Despite advances, for high-current and high-capacity (thick electrode) applications, it is still the ionic conductivity within the solid electrolyte and across the electrolyte/electrode interface that is the main impediment to competitive bulk solid-state cells[8,76].

Wet (solvent-based) methods can also present advantages in terms of the area of solid–solid contact in a solid-state cell. This stems naturally from the increased wettability of a liquid onto a solid, which is converted to active solid–solid interfaces on drying[73]. Indeed, most protective coatings for cathode materials are initiated from a liquid precursor, based on a volatile solvent, which is later evaporated[70,95]. Apart from nanometric coatings, solid electrolytes can be integrated in a solid-state battery directly from liquid suspensions or solutions, forming self-assembled films as shown for Li_3PS_4 from acetonitrile[122]. Slurry processing can ensure good mixing of the various components of composite electrodes (solid electrolyte, active material, conductive carbon, binders) as demonstrated for both sulfide[123] and oxide-based batteries[124]. Such processing routes are closer to well-established process flow of Li-ion battery electrode manufacturing, in which composite sheet electrodes are infiltrated with a liquid electrolyte[73]. It was also shown to be possible to perform the synthesis and integration of a $Li_7P_2S_8I/LiNi_{1/3}Mn_{1/3}Co_{1/3}O_2$ electrode in a single-step by drying a solution of $Li_2S–P_2S_5–LiI–LiNi_{1/3}Mn_{1/3}Co_{1/3}O_2$ reagents[125].

An interesting approach that was demonstrated recently for the low-melting anti-perovskite Li_2OHCl is melt casting, that is, the direct solidification of the solid electrolyte into the desired shape and thickness[126]. In analogy with soft chemistry, melt casting could promote intimate solid–solid ionic contacts but its application is limited to solid electrolyte candidates forming stable melts at low temperatures.

Finally, a critical parameter for the complete processing chain is the ambient stability of reagents and products, which dictates the synthesis environment required and consequently, the potential for scale-up. In particular, sulfides were thought to be intrinsically unstable in ambient humidity, releasing toxic H_2S. However, considerations based on hard/soft-acid/base concepts have led to sulfide electrolytes that are air stable and even water-processable, an example being Na_3SbS_4 (ref. [127]). Similarly, a number of oxide materials (for example, $Li_7La_3Zr_2O_{12}$ and LISICONs) are also prone to degradation in ambient conditions through hydration, protonation and/or CO_2 capture, with the formation of carbonates[24,128].

Conclusions and future outlook

We have highlighted recent progress in the fundamental understanding of solid electrolytes that are relevant to solid-state battery applications. Key properties of solid electrolytes are addressed in the areas of multiscale ion transport, electrochemical and mechanical stabilities, and their reliance on the processing methods available. In many of these areas, deeper insights have been achieved through a close synergy between experimental and modelling techniques. In addition to the major issues covered in this Review, future studies are likely to encompass the following important areas.

Materials discovery. There will be continuing efforts to explore new compounds and structure types that support fast-ion conductivity. The use of high-throughput computational techniques together with experiments will help to identify new candidate compounds. As well as modifying known electrode materials that are successful in liquid-based batteries, we should explore novel electrode materials and protective coatings that are better suited to solid-state battery application including electrode materials exhibiting low and isotropic volumetric expansion on cycling.

Materials and interfacial characterization. In addition to crystallographic studies of the average structure, there will be increasing use of atomic-scale characterization and modelling techniques to probe local structures, ion conduction mechanisms and interfacial chemistry. Key interface issues include greater understanding of grain boundaries and electrolyte/electrode interfacial reactions and kinetics. Critical for the progress of solid-state devices will be the identification of self-passivating solid electrolytes forming stable interfaces with the electrodes or protective coating materials. Novel experimental approaches will need to be designed to monitor solid-state battery operation (preferably operando and in situ), with regard to probing interfacial reactions and pressure evolution.

Materials processing and device operation. There are still many strategies to explore to further optimize both new and conventional electrolyte materials, such as chemical doping, novel synthesis/processing routes and dense thin-film preparation. Technical challenges to be addressed include developing highly scalable routes for synthesis and tailoring mechanical properties for stable operation of solid-state devices. The definition of reproducible protocols setting standards in the synthesis of solid electrolytes and the assembly and cycling of solid-state batteries are crucial for the success of this technology.

Received: 31 October 2018; Accepted: 13 June 2019;
Published online: 19 August 2019

References

1. Placke, T., Kloepsch, R., Dühnen, S. & Winter, M. Lithium ion, lithium metal, and alternative rechargeable battery technologies: the odyssey for high energy density. *J. Solid State Electrochem.* **21**, 1939–1964 (2017).
2. Janek, J. & Zeier, W. G. A solid future for battery development. *Nat. Energy* **1**, 16141 (2016).
3. Inoue, T. & Mukai, K. Are all-solid-state lithium-ion batteries really safe? Verification by differential scanning calorimetry with an all-inclusive microcell. *ACS Appl. Mater. Interfaces* **9**, 1507–1515 (2017).
4. Li, J., Ma, C., Chi, M., Liang, C. & Dudney, N. J. Solid electrolyte: the key for high-voltage lithium batteries. *Adv. Energy Mater.* **5**, 1401408 (2015).
5. Bartsch, T. et al. Gas evolution in all-solid-state battery cells. *ACS Energy Lett.* **3**, 2539–2543 (2018).
6. Luntz, A. C., Voss, J. & Reuter, K. Interfacial challenges in solid-state li ion batteries. *J. Phys. Chem. Lett.* **6**, 4599–4604 (2015).
7. Kato, Y. et al. High-power all-solid-state batteries using sulfide superionic conductors. *Nat. Energy* **1**, 16030 (2016).
8. Kato, Y. et al. All-solid-state batteries with thick electrode configurations. *J. Phys. Chem. Lett.* **9**, 607–613 (2018).
9. Yoshima, K., Harada, Y. & Takami, N. Thin hybrid electrolyte based on garnet-type lithium-ion conductor $Li_7La_3Zr_2O_{12}$ for 12 V-class bipolar batteries. *J. Power Sources* **302**, 283–290 (2016).
10. Albertus, P., Babinec, S., Litzelman, S. & Newman, A. Status and challenges in enabling the lithium metal electrode for high-energy and low-cost rechargeable batteries. *Nat. Energy* **3**, 16–21 (2018).
11. Bai, P., Li, J., Brushett, F. R. & Bazant, M. Z. Transition of lithium growth mechanisms in liquid electrolytes. *Energy Environ. Sci.* **9**, 3221–3229 (2016).
12. Porz, L. et al. Mechanism of lithium metal penetration through inorganic solid electrolytes. *Adv. Energy Mater.* **7**, 1701003 (2017).
13. Zhang, W. et al. (Electro)chemical expansion during cycling: monitoring the pressure changes in operating solid-state lithium batteries. *J. Mater. Chem. A* **5**, 9929–9936 (2017).
14. Koerver, R. et al. Chemo-mechanical expansion of lithium electrode materials — on the route to mechanically optimized all-solid-state batteries. *Energy Environ. Sci.* **11**, 2142–2158 (2018).
15. Koerver, R. et al. Capacity fade in solid-state batteries: interphase formation and chemomechanical processes in nickel-rich layered oxide cathodes and lithium thiophosphate solid electrolytes. *Chem. Mater.* **29**, 5574–5582 (2017).
16. Bucci, G., Talamini, B., Renuka Balakrishna, A., Chiang, Y.-M. & Carter, W. C. Mechanical instability of electrode–electrolyte interfaces in solid-state batteries. *Phys. Rev. Mater.* **2**, 105407 (2018).
17. Jansen, M. Volume effect or paddle-wheel mechanism — fast alkali-metal ionic conduction in solids with rotationally disordered complex anions. *Angew. Chem. Int. Ed.* **30**, 1547–1558 (1991).
18. Wang, Y. et al. Design principles for solid-state lithium superionic conductors. *Nat. Mater.* **14**, 1026–1031 (2015).
19. Le Van-Jodin, L., Ducroquet, F., Sabary, F. & Chevalier, I. Dielectric properties, conductivity and Li^+ ion motion in LiPON thin films. *Solid State Ion.* **253**, 151–156 (2013).
20. Zhu, Z., Chu, I.-H., Deng, Z. & Ong, S. P. Role of Na^+ interstitials and dopants in enhancing the Na^+ conductivity of the cubic Na_3PS_4 superionic conductor. *Chem. Mater.* **27**, 8318–8325 (2015).
21. De Klerk, N. J. J. & Wagemaker, M. Diffusion mechanism of the sodium-ion solid electrolyte Na_3PS_4 and potential improvements of halogen doping. *Chem. Mater.* **28**, 3122–3130 (2016).
22. Tanibata, N., Noi, K., Hayashi, A. & Tatsumisago, M. Preparation and characterization of highly sodium ion conducting Na_3PS_4–Na_4SiS_4 solid electrolytes. *RSC Adv.* **4**, 17120–17123 (2014).
23. Chu, I.-H. et al. Room-temperature all-solid-state rechargeable sodium-ion batteries with a Cl-doped Na_3PS_4 superionic conductor. *Sci. Rep.* **6**, 33733 (2016).
24. Deng, Y. et al. Structural and mechanistic insights into fast lithium-ion conduction in Li_4SiO_4–Li_3PO_4 solid electrolytes. *J. Am. Chem. Soc.* **137**, 9136–9145 (2015).
25. Deng, Y. et al. Enhancing the lithium ion conductivity in lithium superionic conductor (LISICON) solid electrolytes through a mixed polyanion effect. *ACS Appl. Mater. Interfaces* **9**, 7050–7058 (2017).
26. He, X., Zhu, Y. & Mo, Y. Origin of fast ion diffusion in super-ionic conductors. *Nat. Commun.* **8**, 15893 (2017).
27. Burbano, M., Carlier, D., Boucher, F., Morgan, B. J. & Salanne, M. Sparse cyclic excitations explain the low ionic conductivity of stoichiometric $Li_7La_3Zr_2O_{12}$. *Phys. Rev. Lett.* **116**, 135901 (2016).
28. Kanno, R. & Murayama, M. Lithium ionic conductor thio-LISICON: the Li_2S-GeS_2-P_2S_5 system. *J. Electrochem. Soc.* **148**, A742–A746 (2001).
29. Kraft, M. A. et al. Influence of lattice polarizability on the ionic conductivity in the lithium superionic argyrodites Li_6PS_5X (X = Cl, Br, I). *J. Am. Chem. Soc.* **139**, 10909–10918 (2017).
30. Krauskopf, T. et al. Comparing the descriptors for investigating the influence of lattice dynamics on ionic transport using the superionic conductor $Na_3PS_{4-x}Se_x$. *J. Am. Chem. Soc.* **140**, 14464–14473 (2018).
31. Muy, S. et al. Tuning mobility and stability of lithium ion conductors based on lattice dynamics. *Energy Environ. Sci.* **11**, 850–859 (2018).
32. Adams, S. & Prasada Rao, R. Structural requirements for fast lithium ion migration in $Li_{10}GeP_2S_{12}$. *J. Mater. Chem.* **22**, 7687–7691 (2012).
33. Fang, H. & Jena, P. Li-rich antiperovskite superionic conductors based on cluster ions. *Proc. Natl Acad. Sci. USA* **114**, 11046–11051 (2017).
34. Dawson, J. A. et al. Elucidating lithium-ion and proton dynamics in anti-perovskite solid electrolytes. *Energy Environ. Sci.* **11**, 2993–3002 (2018).
35. Tang, W. S. et al. Unparalleled lithium and sodium superionic conduction in solid electrolytes with large monovalent cage-like anions. *Energy Environ. Sci.* **8**, 3637–3645 (2015).
36. Dimitrievska, M. et al. Carbon incorporation and anion dynamics as synergistic drivers for ultrafast diffusion in superionic $LiCB_{11}H_{12}$ and $NaCB_{11}H_{12}$. *Adv. Energy Mater.* **8**, 1703422 (2018).
37. Pecher, O., Carretero-González, J., Griffith, K. J. & Grey, C. P. Materials' methods: NMR in battery research. *Chem. Mater.* **29**, 213–242 (2017).
38. He, X., Zhu, Y., Epstein, A. & Mo, Y. Statistical variances of diffusional properties from ab initio molecular dynamics simulations. *npj Comput. Mater.* **4**, 18 (2018).
39. Marcolongo, A. & Marzari, N. Ionic correlations and failure of Nernst–Einstein relation in solid-state electrolytes. *Phys. Rev. Mater.* **1**, 025402 (2017).
40. Chandra, A., Bhatt, A. & Chandra, A. Ion conduction in superionic glassy electrolytes: an overview. *J. Mater. Sci. Technol.* **29**, 193–208 (2013).
41. Bunde, A., Funke, K. & Ingram, M. D. Ionic glasses: history and challenges. *Solid State Ion.* **105**, 1–13 (1998).
42. Billinge, S. J. L. & Kanatzidis, M. G. Beyond crystallography: the study of disorder, nanocrystallinity and crystallographically challenged materials with pair distribution functions. *Chem. Commun.* **2004**, 749–760 (2004).
43. Mori, K. et al. Structural origin of massive improvement in Li-ion conductivity on transition from $(Li_2S)_5(GeS_2)(P_2S_5)$ glass to $Li_{10}GeP_2S_{12}$ crystal. *Solid State Ion.* **301**, 163–169 (2017).
44. Adams, S. & Swenson, J. Bond valence analysis of reverse Monte Carlo produced structural models; a way to understand ion conduction in glasses. *J. Phys. Condens. Matter.* **17**, S87–S101 (2005).
45. Dietrich, C. et al. Lithium ion conductivity in Li_2S–P_2S_5 glasses — building units and local structure evolution during the crystallization of superionic conductors Li_3PS_4, $Li_7P_3S_{11}$ and $Li_4P_2S_7$. *J. Mater. Chem. A* **5**, 18111–18119 (2017).
46. Lacivita, V. et al. Resolving the amorphous structure of lithium phosphorus oxynitride (LiPON). *J. Am. Chem. Soc.* **140**, 11029–11038 (2018).
47. Li, W., Ando, Y., Minamitani, E. & Watanabe, S. Study of Li atom diffusion in amorphous Li_3PO_4 with neural network potential. *J. Chem. Phys.* **147**, 214106 (2017).
48. Liu, Z. et al. Anomalous high ionic conductivity of nanoporous β-Li_3PS_4. *J. Am. Chem. Soc.* **135**, 975–978 (2013).

49. Tsukasaki, H., Mori, S., Morimoto, H., Hayashi, A. & Tatsumisago, M. Direct observation of a non-crystalline state of Li_2S–P_2S_5 solid electrolytes. *Sci. Rep.* **7**, 4142 (2017).
50. Breuer, S., Uitz, M. & Wilkening, H. M. R. Rapid Li ion dynamics in the interfacial regions of nanocrystalline solids. *J. Phys. Chem. Lett.* **9**, 2093–2097 (2018).
51. Wu, J.-F. & Guo, X. Origin of the low grain boundary conductivity in lithium ion conducting perovskites: $Li_{3x}La_{0.67-x}TiO_3$. *Phys. Chem. Chem. Phys.* **19**, 5880–5887 (2017).
52. Dawson, J. A., Canepa, P., Famprikis, T., Masquelier, C. & Islam, M. S. Atomic-scale influence of grain boundaries on Li-ion conduction in solid electrolytes for all-solid-state batteries. *J. Am. Chem. Soc.* **140**, 362–368 (2018).
53. Ma, C. et al. Atomic-scale origin of the large grain-boundary resistance in perovskite Li-ion-conducting solid electrolytes. *Energy Environ. Sci.* **7**, 1638–1642 (2014).
54. Ganapathy, S., Yu, C., van Eck, E. R. H. & Wagemaker, M. Peeking across grain boundaries in a solid-state ionic conductor. *ACS Energy Lett.* **4**, 1092–1097 (2019).
55. Kim, Y. et al. The effect of relative density on the mechanical properties of hot-pressed cubic $Li_7La_3Zr_2O_{12}$. *J. Am. Ceram. Soc.* **99**, 1367–1374 (2016).
56. Kudu, Ö. U. et al. A review of structural properties and synthesis methods of solid electrolyte materials in the Li_2S–P_2S_5 binary system. *J. Power Sources* **407**, 31–43 (2018).
57. Hayashi, A., Hama, S., Morimoto, H., Tatsumisago, M. & Minami, T. Preparation of Li_2S–P_2S_5 amorphous solid electrolytes by mechanical milling. *J. Am. Ceram. Soc.* **84**, 477–479 (2004).
58. Sakuda, A., Hayashi, A. & Tatsumisago, M. Sulfide solid electrolyte with favorable mechanical property for all-solid-state lithium battery. *Sci. Rep.* **3**, 2261 (2013).
59. Duchardt, M., Ruschewitz, U., Adams, S., Dehnen, S. & Roling, B. Vacancy-controlled Na^+ superion conduction in $Na_{11}Sn_2PS_{12}$. *Angew. Chem. Int. Ed.* **57**, 1351–1355 (2018).
60. Zhang, Z. et al. $Na_{11}Sn_2PS_{12}$: a new solid state sodium superionic conductor. *Energy Environ. Sci.* **11**, 87–93 (2018).
61. Canepa, P. et al. High magnesium mobility in ternary spinel chalcogenides. *Nat. Commun.* **8**, 1759 (2017).
62. Bachman, J. C. et al. Inorganic solid-state electrolytes for lithium batteries: mechanisms and properties governing ion conduction. *Chem. Rev.* **116**, 140–162 (2016).
63. Zhang, Z. et al. New horizons for inorganic solid state ion conductors. *Energy Environ. Sci.* **11**, 1945–1976 (2018).
64. Auvergniot, J. et al. Interface stability of argyrodite Li_6PS_5Cl toward $LiCoO_2$, $LiNi_{1/3}Co_{1/3}Mn_{1/3}O_2$, and $LiMn_2O_4$ in bulk all-solid-state batteries. *Chem. Mater.* **29**, 3883–3890 (2017).
65. Richards, W. D., Miara, L. J., Wang, Y., Kim, J. C. & Ceder, G. Interface stability in solid-state batteries. *Chem. Mater.* **28**, 266–273 (2016).
66. Sakuda, A., Hayashi, A. & Tatsumisago, M. Interfacial observation between $LiCoO_2$ electrode and Li_2S–P_2S_5 solid electrolytes of all-solid-state lithium secondary batteries using transmission electron microscopy. *Chem. Mater.* **22**, 949–956 (2010).
67. Yu, C. et al. Accessing the bottleneck in all-solid state batteries, lithium-ion transport over the solid-electrolyte-electrode interface. *Nat. Commun.* **8**, 1086 (2017).
68. Bielefeld, A., Weber, D. A. & Janek, J. Microstructural modeling of composite cathodes for all-solid-state batteries. *J. Phys. Chem. C* **123**, 1626–1634 (2019).
69. Bron, P., Roling, B. & Dehnen, S. Impedance characterization reveals mixed conducting interphases between sulfidic superionic conductors and lithium metal electrodes. *J. Power Sources* **352**, 127–134 (2017).
70. Zhang, W. et al. Interfacial processes and influence of composite cathode microstructure controlling the performance of all-solid-state lithium batteries. *ACS Appl. Mater. Interfaces* **9**, 17835–17845 (2017).
71. Wenzel, S., Sedlmaier, S. J., Dietrich, C., Zeier, W. G. & Janek, J. Interfacial reactivity and interphase growth of argyrodite solid electrolytes at lithium metal electrodes. *Solid State Ion.* **318**, 102–112 (2018).
72. Nam, Y. J., Oh, D. Y., Jung, S. H. & Jung, Y. S. Toward practical all-solid-state lithium-ion batteries with high energy density and safety: comparative study for electrodes fabricated by dry- and slurry-mixing processes. *J. Power Sources* **375**, 93–101 (2018).
73. Kim, D. H. et al. Infiltration of solution-processable solid electrolytes into conventional Li-ion-battery electrodes for all-solid-state Li-ion batteries. *Nano Lett.* **17**, 3013–3020 (2017).
74. Braun, P., Uhlmann, C., Weiss, M., Weber, A. & Ivers-Tiffée, E. Assessment of all-solid-state lithium-ion batteries. *J. Power Sources* **393**, 119–127 (2018).
75. Froboese, L., van der Sichel, J. F., Loellhoeffel, T., Helmers, L. & Kwade, A. Effect of microstructure on the ionic conductivity of an all solid-state battery electrode. *J. Electrochem. Soc.* **166**, A318–A328 (2019).
76. Strauss, F. et al. Impact of cathode material particle size on the capacity of bulk-type all-solid-state batteries. *ACS Energy Lett.* **3**, 992–996 (2018).
77. Haruyama, J., Sodeyama, K., Han, L., Takada, K. & Tateyama, Y. Space-charge layer effect at interface between oxide cathode and sulfide electrolyte in all-solid-state lithium-ion battery. *Chem. Mater.* **26**, 4248–4255 (2014).
78. de Klerk, N. J. J. & Wagemaker, M. Space-charge layers in all-solid-state batteries; important or negligible? *ACS Appl. Energy Mater.* **1**, 5609–5618 (2018).
79. Sang, L., Haasch, R. T., Gewirth, A. A. & Nuzzo, R. G. Evolution at the solid electrolyte/gold electrode interface during lithium deposition and stripping. *Chem. Mater.* **29**, 3029–3037 (2017).
80. Zhu, Y., He, X. & Mo, Y. Origin of outstanding stability in the lithium solid electrolyte materials: insights from thermodynamic analyses based on first-principles calculations. *ACS Appl. Mater. Interfaces* **7**, 23685–23693 (2015).
81. Swamy, T., Chen, X. & Chiang, Y.-M. Electrochemical redox behavior of li ion conducting sulfide solid electrolytes. *Chem. Mater.* **31**, 707–713 (2019).
82. Han, F., Gao, T., Zhu, Y., Gaskell, K. J. & Wang, C. A battery made from a single material. *Adv. Mater.* **27**, 3473–3483 (2015).
83. Tian, Y. et al. Compatibility issues between electrodes and electrolytes in solid-state batteries. *Energy Environ. Sci.* **10**, 1150–1166 (2017).
84. Tang, H. et al. Probing solid–solid interfacial reactions in all-solid-state sodium-ion batteries with first-principles calculations. *Chem. Mater.* **30**, 163–173 (2018).
85. Chen, T., Ceder, G., Sai Gautam, G. & Canepa, P. Evaluation of Mg compounds as coating materials in Mg batteries. *Front. Chem.* **7**, 1–10 (2019).
86. Maier, J. in *Handbook of Solid State Chemistry* (eds Dronskowski, R., Kikkawa, S. & Stein, A.) 665–701 (Wiley, 2017).
87. Lu, Z. & Ciucci, F. Metal borohydrides as electrolytes for solid-state Li, Na, Mg, and Ca batteries: a first-principles study. *Chem. Mater.* **29**, 9308–9319 (2017).
88. Hartmann, P. et al. Degradation of NASICON-type materials in contact with lithium metal: formation of mixed conducting interphases (MCI) on solid electrolytes. *J. Phys. Chem. C* **117**, 21064–21074 (2013).
89. Wenzel, S. et al. Direct observation of the interfacial instability of the fast ionic conductor $Li_{10}GeP_2S_{12}$ at the lithium metal anode. *Chem. Mater.* **28**, 2400–2407 (2016).
90. Sakuma, M., Suzuki, K., Hirayama, M. & Kanno, R. Reactions at the electrode/electrolyte interface of all-solid-state lithium batteries incorporating Li–M (M = Sn, Si) alloy electrodes and sulfide-based solid electrolytes. *Solid State Ion.* **285**, 101–105 (2016).
91. Wenzel, S. et al. Interfacial reactivity benchmarking of the sodium ion conductors Na_3PS_4 and sodium β-alumina for protected sodium metal anodes and sodium all-solid-state batteries. *ACS Appl. Mater. Interfaces* **8**, 28216–28224 (2016).
92. Ma, C. et al. Interfacial stability of Li metal–solid electrolyte elucidated via in situ electron microscopy. *Nano Lett.* **16**, 7030–7036 (2016).
93. Rettenwander, D. et al. Interface instability of Fe-stabilized $Li_7La_3Zr_2O_{12}$ versus Li metal. *J. Phys. Chem. C* **122**, 3780–3785 (2018).
94. Schwöbel, A., Hausbrand, R. & Jaegermann, W. Interface reactions between LiPON and lithium studied by in-situ X-ray photoemission. *Solid State Ion.* **273**, 51–54 (2015).
95. Ohta, N. et al. Enhancement of the high-rate capability of solid-state lithium batteries by nanoscale interfacial modification. *Adv. Mater.* **18**, 2226–2229 (2006).
96. Jung, S. H. et al. Li_3BO_3–Li_2CO_3: rationally designed buffering phase for sulfide all-solid-state Li-ion batteries. *Chem. Mater.* **30**, 8190–8200 (2018).
97. Koerver, R. et al. Redox-active cathode interphases in solid-state batteries. *J. Mater. Chem. A* **5**, 22750–22760 (2017).
98. Shin, B. R. et al. Comparative Study of TiS_2/Li-In all-solid-state lithium batteries using glass-ceramic Li_3PS_4 and $Li_{10}GeP_2S_{12}$ solid electrolytes. *Electrochim. Acta* **146**, 395–402 (2014).
99. Hakari, T. et al. Structural and electronic-state changes of a sulfide solid electrolyte during the Li deinsertion–insertion processes. *Chem. Mater.* **29**, 4768–4774 (2017).
100. Schafzahl, L. et al. Long-chain Li and Na alkyl carbonates as solid electrolyte interphase components: structure, ion transport, and mechanical properties. *Chem. Mater.* **30**, 3338–3345 (2018).
101. Dietrich, C. et al. Spectroscopic characterization of lithium thiophosphates by XPS and XAS — a model to help monitor interfacial reactions in all-solid-state batteries. *Phys. Chem. Chem. Phys.* **20**, 20088–20095 (2018).
102. Lorger, S., Usiskin, R. E. & Maier, J. Transport and charge carrier chemistry in lithium sulfide. *Adv. Funct. Mater.* **29**, 1807688 (2018).
103. Zhu, Y., He, X. & Mo, Y. First principles study on electrochemical and chemical stability of solid electrolyte–electrode interfaces in all-solid-state Li-ion batteries. *J. Mater. Chem. A* **4**, 3253–3266 (2016).
104. Wu, X., El Kazzi, M. & Villevieille, C. Surface and morphological investigation of the electrode/electrolyte properties in an all-solid-state battery using a Li_2S–P_2S_5 solid electrolyte. *J. Electroceram.* **38**, 207–214 (2017).
105. Zhao, Y. et al. A review on modeling of electro-chemo-mechanics in lithium-ion batteries. *J. Power Sources* **413**, 259–283 (2019).

106. Han, X. et al. Negating interfacial impedance in garnet-based solid-state Li metal batteries. *Nat. Mater.* **16**, 572–579 (2016).
107. Wang, M. & Sakamoto, J. Correlating the interface resistance and surface adhesion of the Li metal–solid electrolyte interface. *J. Power Sources* **377**, 7–11 (2018).
108. McGrogan, F. P. et al. Compliant yet brittle mechanical behavior of Li_2S-P_2S_5 lithium-ion-conducting solid electrolyte. *Adv. Energy Mater.* **7**, 1602011 (2017).
109. Bucci, G., Swamy, T., Chiang, Y.-M. & Carter, W. C. Modeling of internal mechanical failure of all-solid-state batteries during electrochemical cycling, and implications for battery design. *J. Mater. Chem. A* **5**, 19422–19430 (2017).
110. Deng, Z., Wang, Z., Chu, I.-H., Luo, J. & Ong, S. P. Elastic properties of alkali superionic conductor electrolytes from first principles calculations. *J. Electrochem. Soc.* **163**, A67–A74 (2016).
111. Bo, S.-H., Wang, Y. & Ceder, G. Structural and Na-ion conduction characteristics of $Na_3PS_xSe_{4-x}$. *J. Mater. Chem. A* **4**, 9044–9053 (2016).
112. Geiger, C. A. et al. Crystal chemistry and stability of "$Li_7La_3Zr_2O_{12}$" garnet: a fast lithium-ion conductor. *Inorg. Chem.* **50**, 1089–1097 (2011).
113. Boulineau, S., Courty, M., Tarascon, J. M. & Viallet, V. Mechanochemical synthesis of Li-argyrodite Li_6PS_5X (X = Cl, Br, I) as sulfur-based solid electrolytes for all solid state batteries application. *Solid State Ion.* **221**, 1–5 (2012).
114. Hayashi, A., Noi, K., Sakuda, A. & Tatsumisago, M. Superionic glass-ceramic electrolytes for room-temperature rechargeable sodium batteries. *Nat. Commun.* **3**, 856 (2012).
115. Kuhn, A. et al. A new ultrafast superionic Li-conductor: ion dynamics in $Li_{11}Si_2PS_{12}$ and comparison with other tetragonal LGPS-type electrolytes. *Phys. Chem. Chem. Phys.* **16**, 14669–14674 (2014).
116. Yi, E., Wang, W., Kieffer, J. & Laine, R. M. Key parameters governing the densification of cubic-$Li_7La_3Zr_2O_{12}$ Li^+ conductors. *J. Power Sources* **352**, 156–164 (2017).
117. Delaizir, G. et al. The stone age revisited: building a monolithic inorganic lithium-ion battery. *Adv. Funct. Mater.* **22**, 2140–2147 (2012).
118. Schnell, J. et al. All-solid-state lithium-ion and lithium metal batteries — paving the way to large-scale production. *J. Power Sources* **382**, 160–175 (2018).
119. Oudenhoven, J. F. M., Baggetto, L. & Notten, P. H. L. All-solid-state lithium-ion microbatteries: a review of various three-dimensional concepts. *Adv. Energy Mater.* **1**, 10–33 (2011).
120. Hitz, G. T. et al. High-rate lithium cycling in a scalable trilayer Li-garnet-electrolyte architecture. *Mater. Today* **22**, 50–57 (2019).
121. Wang, D. et al. Mitigating the interfacial degradation in cathodes for high-performance oxide-based solid-state lithium batteries. *ACS Appl. Mater. Interfaces* **11**, 4954–4961 (2019).
122. Wang, H., Hood, Z. D., Xia, Y. & Liang, C. Fabrication of ultrathin solid electrolyte membranes of β-Li_3PS_4 nanoflakes by evaporation-induced self-assembly for all-solid-state batteries. *J. Mater. Chem. A* **4**, 8091–8096 (2016).
123. Ates, T., Keller, M., Kulisch, J., Adermann, T. & Passerini, S. Development of an all-solid-state lithium battery by slurry-coating procedures using a sulfidic electrolyte. *Energy Storage Mater.* **17**, 204–210 (2018).
124. Finsterbusch, M. et al. High Capacity garnet-based all-solid-state lithium batteries: fabrication and 3D-microstructure resolved modeling. *ACS Appl. Mater. Interfaces* **10**, 22329–22339 (2018).
125. Matsuda, R., Hirabara, E., Phuc, N. H. H., Muto, H. & Matsuda, A. Composite cathode of NCM particles and Li_3PS_4–LiI electrolytes prepared using the SEED method for all-solid-state lithium batteries. *IOP Conf. Ser. Mater. Sci. Eng.* **429**, 012033 (2018).
126. Hood, Z. D., Wang, H., Samuthira Pandian, A., Keum, J. K. & Liang, C. Li_2OHCl crystalline electrolyte for stable metallic lithium anodes. *J. Am. Chem. Soc.* **138**, 1768–1771 (2016).
127. Kim, T. W., Park, K. H., Choi, Y. E., Lee, J. Y. & Jung, Y. S. Aqueous-solution synthesis of Na_3SbS_4 solid electrolytes for all-solid-state Na-ion batteries. *J. Mater. Chem. A* **6**, 840–844 (2018).
128. Sharafi, A. et al. Impact of air exposure and surface chemistry on Li–$Li_7La_3Zr_2O_{12}$ interfacial resistance. *J. Mater. Chem. A* **5**, 13475–13487 (2017).
129. Groh, M. F. et al. Interface instability in $LiFePO_4$–$Li_{3+x}P_{1-x}Si_xO_4$ all-solid-state batteries. *Chem. Mater.* **30**, 5886–5895 (2018).
130. Wu, X., Villevieille, C., Novák, P. & El Kazzi, M. Monitoring the chemical and electronic properties of electrolyte–electrode interfaces in all-solid-state batteries using operando X-ray photoelectron spectroscopy. *Phys. Chem. Chem. Phys.* **20**, 11123–11129 (2018).
131. Chen, K. et al. Morphological effect on reaction distribution influenced by binder materials in composite electrodes for sheet-type all-solid-state lithium-ion batteries with the sulfide-based solid electrolyte. *J. Phys. Chem. C* **123**, 3292–3298 (2019).
132. Park, K. et al. Electrochemical nature of the cathode interface for a solid-state lithium-ion battery: interface between $LiCoO_2$ and garnet-$Li_7La_3Zr_2O_{12}$. *Chem. Mater.* **28**, 8051–8059 (2016).
133. Walther, F. et al. Visualization of the interfacial decomposition of composite cathodes in argyrodite-based all-solid-state batteries using time-of-flight secondary-ion mass spectrometry. *Chem. Mater.* **31**, 3745–3755 (2019).
134. Zhang, W. et al. Degradation mechanisms at the $Li_{10}GeP_2S_{12}$/$LiCoO_2$ cathode interface in an all-solid-state lithium-ion battery. *ACS Appl. Mater. Interfaces* **10**, 22226–22236 (2018).
135. Wang, C. et al. In situ neutron depth profiling of lithium metal–garnet interfaces for solid state batteries. *J. Am. Chem. Soc.* **139**, 14257–14264 (2017).
136. Han, F. et al. High electronic conductivity as the origin of lithium dendrite formation within solid electrolytes. *Nat. Energy* **4**, 187–196 (2019).
137. Shen, F., Dixit, M. B., Xiao, X. & Hatzell, K. B. Effect of pore connectivity on Li dendrite propagation within LLZO electrolytes observed with synchrotron X-ray tomography. *ACS Energy Lett.* **3**, 1056–1061 (2018).
138. Cheng, T., Merinov, B. V., Morozov, S. & Goddard, W. A. Quantum mechanics reactive dynamics study of solid Li-electrode/Li_6PS_5Cl-electrolyte interface. *ACS Energy Lett.* **2**, 1454–1459 (2017).
139. Schnell, J. et al. Prospects on production technologies and manufacturing cost of oxide-based all-solid-state lithium batteries. *Energy Environ. Sci.* **12**, 1818–1833 (2019).
140. De Jonghe, L. C., Feldman, L. & Millett, P. Some geometrical aspects of breakdown of sodium beta alumina. *Mater. Res. Bull.* **14**, 589–595 (1979).
141. Scrosati, B. & Butherus, A. D. Electrochemical Properties of $RbAg_4I_5$ Solid Electrolyte. *J. Electrochem. Soc.* **119**, 128–133 (1972).
142. Sharafi, A. et al. Surface chemistry mechanism of ultra-low interfacial resistance in the solid-state electrolyte $Li_7La_3Zr_2O_{12}$. *Chem. Mater.* **29**, 7961–7968 (2017).
143. Wang, M., Wolfenstine, J. B. & Sakamoto, J. Temperature dependent flux balance of the Li/$Li_7La_3Zr_2O_{12}$ interface. *Electrochim. Acta* **296**, 842–847 (2019).
144. Masias, A., Felten, N., Garcia-Mendez, R., Wolfenstine, J. & Sakamoto, J. Elastic, plastic, and creep mechanical properties of lithium metal. *J. Mater. Sci.* **54**, 2585–2600 (2019).
145. Monroe, C. & Newman, J. The impact of elastic deformation on deposition kinetics at lithium/polymer interfaces. *J. Electrochem. Soc.* **152**, A396–A404 (2005).
146. Ahmad, Z. & Viswanathan, V. Stability of electrodeposition at solid-solid interfaces and implications for metal anodes. *Phys. Rev. Lett.* **119**, 056003 (2017).
147. Yu, S. et al. Elastic properties of the solid electrolyte $Li_7La_3Zr_2O_{12}$ (LLZO). *Chem. Mater.* **28**, 197–206 (2016).
148. Ahmad, Z., Xie, T., Maheshwari, C., Grossman, J. C. & Viswanathan, V. Machine learning enabled computational screening of inorganic solid electrolytes for suppression of dendrite formation in lithium metal anodes. *ACS Cent. Sci.* **4**, 996–1006 (2018).
149. Marbella, L. E. et al. ^{7}Li NMR chemical shift imaging to detect microstructural growth of lithium in all-solid-state batteries. *Chem. Mater.* **31**, 2762–2769 (2019).
150. Manalastas, W. et al. Mechanical failure of garnet electrolytes during Li electrodeposition observed by in-operando microscopy. *J. Power Sources* **412**, 287–293 (2019).
151. Han, F., Yue, J., Zhu, X. & Wang, C. Suppressing Li dendrite formation in Li_2S-P_2S_5 solid electrolyte by LiI incorporation. *Adv. Energy Mater.* **8**, 1703644 (2018).

Acknowledgements

T.F. acknowledges the Alistore ERI (http://www.alistore.eu/) and CNRS for their financial support in the form of a joint PhD scholarship between Amiens (France) and Bath (UK). P.C. is grateful to the Ramsey Memorial Trust and the University of Bath for the provision of his Ramsey Fellowship. M.S.I. and J.A.D. gratefully acknowledge the EPSRC Programme Grant (EP/M009521/1). The authors are grateful to D. Efremidis for help with the graphical design for Fig. 1.

Author contributions

T.F., P.C. and J.A.D. carried out the literature review and T.F. drafted the manuscript. All authors contributed to the analysis, discussion and revisions leading to the final version of the manuscript.

Competing interests

The authors declare no competing interests.

Additional information

Reprints and permissions information is available at www.nature.com/reprints.

Correspondence should be addressed to T.F., M.S.I. or C.M.

Publisher's note: Springer Nature remains neutral with regard to jurisdictional claims in published maps and institutional affiliations.